Chemical Geology 296–297 (2012) 103–118

Contents lists available at SciVerse ScienceDirect

Chemical Geology

journal homepage: www.elsevier.com/locate/chemgeo

Research paper

Rare earth element geochemistry of laminated diatom mats from tropical West Pacific: Evidence for more reducing bottomwaters and higher primary productivity during the Last Glacial Maximum

Zhifang Xiong [a], Tiegang Li [a,*], Thomas Algeo [b], Fengming Chang [a], Xuebo Yin [a], Zhaokai Xu [a]

[a] *Key Laboratory of Marine Geology and Environment, Institute of Oceanology, Chinese Academy of Sciences, Qingdao 266071, China*
[b] *Department of Geology, University of Cincinnati, Cincinnati, OH 45221-0013, USA*

ARTICLE INFO

Article history:
Received 6 December 2011
Accepted 8 December 2011
Available online 26 December 2011

Editor: U. Brand

Keywords:
Diatom mats
Rare earth elements
Cerium and europium anomalies
Ethmodiscus rex
West Pacific
Last Glacial Maximum

ABSTRACT

Rare earth elements (REE) along with selected major and trace elements were measured in laminated *Ethmodiscus rex* diatom mats and associated sediments (diatomaceous clay and pelagic clay) in two sediment cores collected from the Parece Vela Basin of the eastern Philippine Sea. REE distributions are characterized by strong enrichment of middle REE (MREE) and heavy REE (HREE) over light REE (LREE) and slight enrichment of MREE over HREE. This distribution pattern suggests that REE compositions of the laminated *E. rex* diatom mats were not the product of *E. rex* blooms, an inference also supported by the fact that Ti-normalized REE concentrations are not clearly different from those in the diatomaceous clay and pelagic clay. Comparison of REE patterns with the vertical distribution of authigenic phases in the sediment indicates that LREE were dominantly associated with detrital materials, whereas MREE and HREE were selectively enriched by Mn oxyhydroxides and authigenic phosphates. In the pelagic clay, a weak negative Ce anomaly cannot be linked to oxic depositional conditions but instead is attributed to the retention of a negative Ce anomaly associated with authigenic phosphates. In the laminated *E. rex* diatom mats, a weak positive Ce anomaly is consistent with depositional sulfidic anoxic conditions and is interpreted to represent enhanced scavenging of reduced aqueous Ce^{3+} by barite in a strongly reducing environment. Moreover, variably negative to positive Ce anomalies in the diatomaceous clay may reflect the concurrent operation of the two processes controlling Ce accumulation in the laminated *E. rex* diatom mats and pelagic clay. The study cores show a ubiquitous positive Eu anomaly owing to the presence of volcanic materials. The smaller Eu anomaly in the laminated *E. rex* diatom mats and diatomaceous clay relative to that in the pelagic clay may be attributed to the release of reduced Eu^{2+} from mineral phases to the sediment pore water under strongly reducing conditions. Previous studies have shown that the advection of Lower Circumpolar Water (LCPW) strengthened during the Last Glacial Maximum (LGM), which should have resulted in better ventilation of the deep eastern Philippine Sea. Evidence presented here for more reducing bottomwater conditions during the laminated *E. rex* diatom mats formation implicates elevated primary productivity and enhanced organic sinking fluxes as primary controls on redox changes in the eastern Philippine Sea during the LGM. Enhanced primary productivity and more reducing bottomwaters during the laminated *E. rex* diatom mats deposition resulted in a larger respired carbon pool in the deep eastern Philippine Sea, which may have been part of a larger-scale modulation of atmospheric CO_2 variation during Pleistocene glacial–interglacial cycles by deep-ocean carbon storage.

1. Introduction

Laminated diatom mats (LDMs), formed by the accumulation of giant and "shade flora" diatoms such as *Ethmodiscus rex*, *Rhizosolenia* spp. and *Thalassiothrix* spp., have been found sporadically in abyssal environments of the global ocean (Kemp et al., 2000, 2006; Romero and Schmieder, 2006). These species are capable of buoyancy regulation, migrating vertically within the water column to exploit nutrients in the sub-photic zone (Villareal, 1993). Blooms in the tropical ocean are generally related to strong oceanic stratification, while blooms in subtropical settings are mainly associated with frontal zones (i.e., interfaces between ocean water masses; Yoder et al., 1994; Gingele and Schmieder, 2001; De Deckker and Gingele, 2002; Gingele et al., 2002). Owing to the massive flux of organic carbon and biogenic silica produced by these mat-forming diatoms to the seafloor, LDMs are likely to play a significant role in the global carbon and silicon cycles (Kemp

---

* Corresponding author.
E-mail address: tgli@qdio.ac.cn (T. Li).

0009-2541/$ – see front matter © 2011 Elsevier B.V. All rights reserved.
doi:10.1016/j.chemgeo.2011.12.012

et al., 2006). However, the origin of LDMs and their role in forcing of global climate change remain poorly understood.

During the Last Glacial Maximum (LGM), laminated *E. rex* mats accumulated widely in the eastern Philippine Sea (Zhai et al., 2009). *E. rex* blooms were probably controlled by changes in stratification and nutrient availability within the intermediate watermass. The LGM coincided with increased advection of Lower Circumpolar Water (LCPW) into the eastern Philippine basin (Veum et al., 1992; McCave et al., 1995; Pudsey and Howe, 1998), which may have enhanced water-column stratification, producing conditions favoring elevated primary productivity by *E. rex*. Advection of LCPW waters is also thought to have increased ventilation of the deep watermass of the eastern Philippine Sea (Siedler et al., 2004), but evidence for intensification of reducing conditions in bottomwaters during the LGM (Xiong et al., in review) suggests that any improvement in ventilation was offset by an increased sinking flux of organic matter associated with diatom blooms.

The rare earth elements (REEs) comprise 14 elements that increase in atomic number from lanthanum (La) to lutetium (Lu), exhibit generally similar geochemical behavior due to their intrinsic chemical properties. In natural environments, all REEs occur in the trivalent state (+3) except for cerium (Ce), which can change its valence to +4 under oxidizing conditions, and europium (Eu), which can change its valence to +2 under reducing conditions (Elderfield and Greaves, 1982; Nozaki, 2009). Apart from redox-controlled fractionation of Ce and Eu, the other REEs show ordered distributions that enable them to be widely employed as geochemical tracers in marine environments. REEs are useful for identifying detrital sediment provenance (Munksgaard et al., 2003), monitoring climate change (Tanaka et al., 2007), investigating diagenetic processes (Caetano et al., 2009), characterizing the chemistry of seawater (Piper et al., 2007), pore water (Haley et al., 2004), and particulate matter (Sholkovitz et al., 1994), and reconstructing aqueous redox state (Morad and Felitsyn, 2001; Jiang et al., 2007) and ocean circulation patterns (Lacan and Jeandel, 2001). The REE geochemistry of LDMs has received little attention to date. In this paper, we present REE data from two late Pleistocene cores collected in the eastern Philippine Sea in order to (1) document REE concentrations and distribution patterns, (2) identify potential carrier phases of REEs, (3) investigate relationships of Ce and Eu anomalies with redox conditions before, during, and after deposition of LDM, and (4) demonstrate the importance of enhanced primary productivity for development of sulfidic anoxic conditions in the eastern Philippine Sea during the LGM. The results of this study provide insights regarding the relationship of mat-forming diatom blooms to the REE geochemistry of marine sediments as well as the use of Ce and Eu anomalies as indicators of paleoredox environments.

2. Materials and methods

2.1. Study cores

LDMs were analyzed for elemental geochemistry in two deep-sea cores from the Parece Vela Basin of the eastern Philippine Sea (Fig. 1): (1) core WPD-03, 405 cm long, recovered during the 2004 cruise of *R/V Science No. 1* in 5250 m water depth at 17°19.82′ N and 138°27.28′ E, and (2) core WPD-12, 100 cm long, obtained during the 2003 cruise of *R/V Science No. 1* in 4954 m water depth at 20°35.95′ N and 139°14.54′ E. Both of the cores contain little carbonate because the study sites lie below the calcium carbonate compensation depth. The longer core (WPD-03) comprises three discrete lithostratigraphic units. The upper unit (0–286 cm) is composed of olive-gray and gray laminated diatom mats (LDM-03), which are dominated by fragmented valves of the mat-forming diatom *E. rex* in near-monospecific assemblages with extremely low abundances of other diatom species and radiolarians (Zhai et al., 2009). The middle unit (286–334 cm) is characterized by gray diatomaceous clays (DC). The lower unit (334–405 cm) comprises massive red pelagic clays (PC). Analysis of redox-sensitive and sulfide-forming elements imply that the LDM-03 and DC were deposited under predominantly suboxic (to rarely sulfidic anoxic) conditions, whereas the PC was deposited under largely oxic conditions (Xiong et al., in review). The shorter core (WPD-12) contains only the laminated diatom mat facies (LDM-12), which resembles the LDM of WPD-03 but contains greater quantities of non-biogenic silica. Siliceous material of non-biogenic origin in eastern Philippine Sea sediments is sourced primarily from alteration of seafloor volcanic materials and secondarily from an Asian eolian dust flux (Xu et al., 2008). AMS^{14}C dates indicate that LDMs in the study area formed during the late Wisconsinan glacial stage (mainly during the Last Glacial Maximum, ~18 to 28 kyr B.P.) (Zhai et al., 2009).

2.2. Analytical procedures

For major, trace and rare earth element analysis, approximately 40 mg of dried and ground sample powders were weighed into a Teflon vessel. After 2 mL HNO_3 and 0.5 mL HF were added to it, the vessel was sealed and allowed to settle for 2 h, and it was then heated overnight (24 h) on hot plates at 150 °C. Later, 0.25 mL $HClO_4$ was added to the open vessel and evaporated to dryness on hot plates at 120 °C. The residue was dissolved in 1 mL HNO_3 + 1 mL H_2O in an airtight vessel for 12 h at 120 °C before being diluted to 40 g with distilled and deionized water. Blanks, duplicate samples, and a suite of USGS and Chinese rock and sediment standards (QLO-2, BCR-2, BHVO-2, GBW07103, GBW07316 and GBW07315) were also prepared by the same method to monitor instrument precision and assess data quality. Major elements (Al, Ti, Fe, Mn, P), a trace element (Ba), and REEs (La to Lu) were determined using a Thermo-Fisher iCAP6300 ICP-OES and a Perkin-Elmer ELAN DRC II ICP-MS, respectively, at the Institute of Oceanology, Chinese Academy of Sciences (IOCAS). Analytical accuracy was assessed by the analysis of selected USGS and Chinese certified reference materials (BCR-2, BHVO-2, GBW07316 and GBW07315), which gave results typically within ±10% of certified values (Table 1; Supplementary Table 1). Analytical precision, given as the relative standard deviation (RSD), was determined by analyses of several duplicate samples and was typically better than 5% for major, trace, and rare earth elements.

Biogenic silica (BSi) was determined using the alkaline extraction method of Mortlock and Froelich (1989), followed by measurement by a Thermo-Fisher iCAP6300 ICP-OES at IOCAS. The values reported here as opal content were calculated as %opal = 2.4 × %BSi, where the coefficient 2.4 accounts for structural water and silica (Mortlock and Froelich, 1989). The analytical precision (RSD), determined by analyses of duplicate samples, was typically better than 9%.

2.3. Data presentation

Elemental concentrations were normalized to the detrital element Ti in order to reduce or remove the dilution effect of opal (see Supplementary Table 2 for large datasets). In the following analysis, we utilize several calculated REE parameters. First, $(Eu/La)_N$, $(Yb/La)_N$ and $(Eu/Yb)_N$ are used to assess the enrichment of MREE relative to LREE, HREE relative to LREE, and MREE relative to HREE, respectively (Taylor and McClennan, 1985; Johannesson et al., 2006); note that the subscript “N” designates elemental concentration ratios normalized to Post-Archean Australian Shale (PAAS) (Taylor and McClennan, 1985). Second, the concentration of “excess REEs” was calculated as follows (Murray et al., 1993):

$$REE_{xs} = REE_{sample} - Ti_{sample} \times (REE/Ti)_{PAAS} \tag{1}$$

where the subscript “xs” indicates excess concentration. Excess REE represents the total concentration of REE minus the estimated detrital

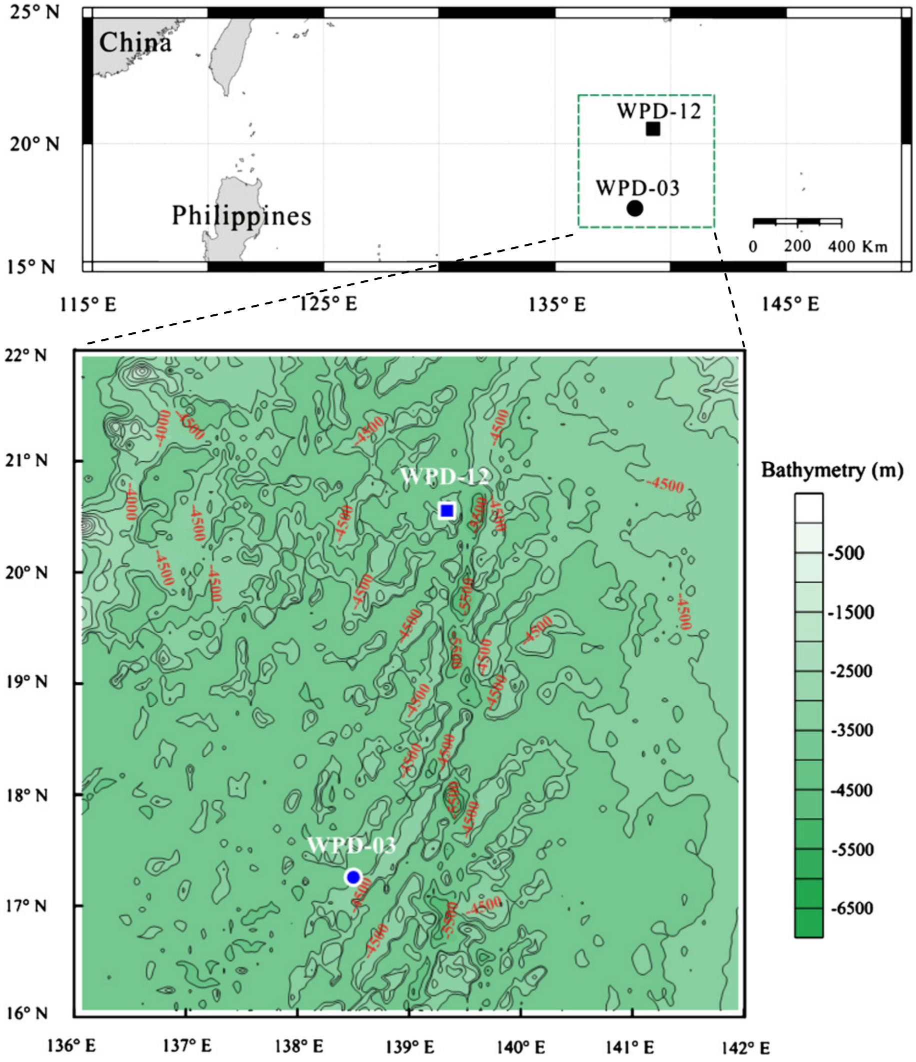

Fig. 1. Locations of the WPD-03 and WPD-12 study cores containing laminated *Ethmodiscus rex* diatom mats (LDM) from the Parece Vela Basin of the eastern Philippine Sea. The base map was drawn using the online map creation program at http://www.aquarius.ifm-geomar.de. The bathymetric data are from http://topex.ucsd.edu/cgi-bin/get_data.cgi.

contribution and, thus, is a proxy for the authigenic fraction of REEs in the sediment.

Third, Ce and Eu anomalies represent the enrichment or depletion of these REEs compared to neighboring elements in the lanthanide series. Due to redox-controlled fractionation, Ce and Eu frequently present distinctive deviations from the regular behavior of the REEs (see Section 3.3.1). These deviations are generally expressed as Ce and Eu anomalies, which are quantified as the ratios of their

Table 1
Measured and certified concentrations of REEs for selected USGS and Chinese certified reference materials.

Elements	Certified reference materials (ppm)							
	BHVO-2		BCR-2		GBW07316		GBW07315	
	Measured	Certified	Measured	Certified	Measured	Certified	Measured	Certified
La	15.67	15	25.52	25	42.37	44	60.63	62
Ce	37.99	38	53.63	53	54.20	55	79.72	82
Pr	5.46	NA[a]	6.96	6.8	11.75	12	17.11	17
Nd	24.48	25	28.80	28	50.15	51	72.68	75
Sm	5.74	6.2	6.38	6.7	11.61	12	17.13	18
Eu	2.68	NA	2.37	2	2.94	3	4.69	4.5
Gd	5.68	6.3	6.44	6.8	11.86	12	17.33	18
Tb	0.96	0.9	1.05	1.07	1.90	2	2.90	3.1
Dy	4.96	NA	6.00	NA	10.50	11	15.98	17
Ho	0.99	1.04	1.32	1.33	2.24	2.4	3.51	3.6
Er	2.40	NA	3.46	NA	5.89	6.3	9.16	9.8
Tm	0.34	NA	0.54	0.54	0.90	0.96	1.43	1.4
Yb	2.00	2	3.31	3.5	5.42	5.8	8.81	8.9
Lu	0.28	0.28	0.50	0.51	0.80	0.89	1.36	1.3

[a] NA: not available.

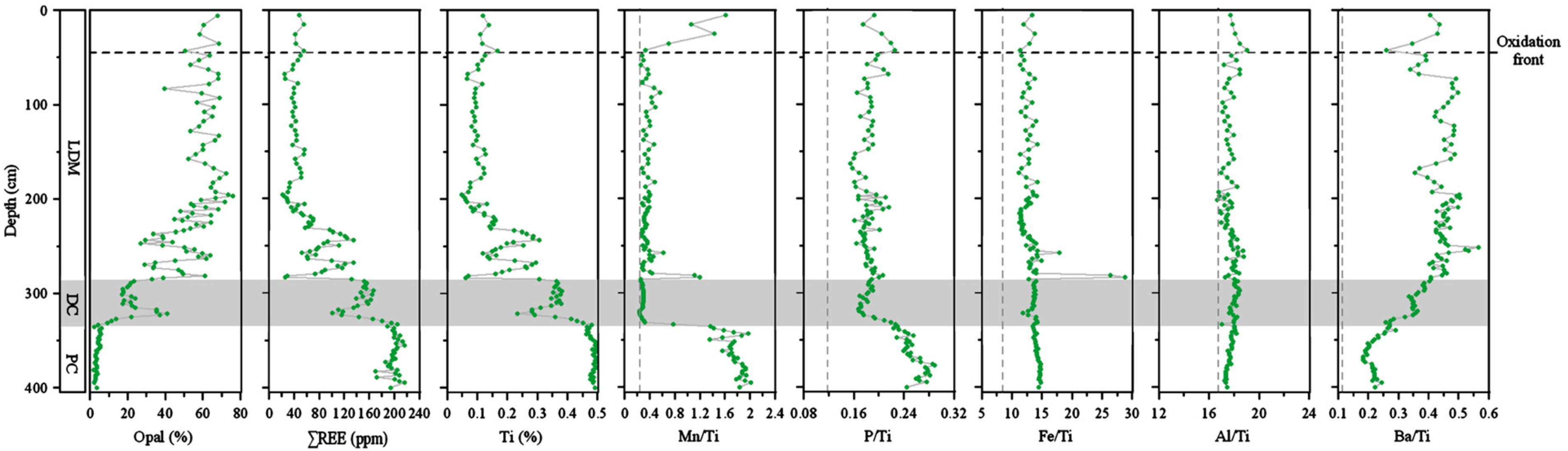

Fig. 2. Depth profiles for the concentration of opal, total rare earth elements (REEs), Ti, Mn/Ti, P/Ti, Fe/Ti, Al/Ti and Ba/Ti ratios in core WPD-03. The vertical dashed lines show element/Ti ratios for PAAS (Taylor and McClennan, 1985). The horizontal dashed line shows the position of the active oxidation front (Xiong et al., in review). LDM: laminated *Ethmodiscus rex* diatom mats; DC: diatomaceous clay; and PC: pelagic clay.

normalized concentrations to the arithmetic mean of respective neighboring trivalent REE (Nozaki, 2009). Unfortunately, the algorithms for calculating Ce and Eu anomalies have not been standardized (Holser, 1997). For analytical reasons Pr sometimes was not reported in the older literature, so the Ce anomaly was calculated using Nd or Sm (Grandjean-Lécuyer et al., 1993; Wilde et al., 1996; Lerche and Nozaki, 1998), e.g.:

$$Ce\ \ anomaly = \log[3Ce_N/(2La_N + Nd_N)] \tag{2}$$

$$Ce\ \ anomaly = \log[5Ce_N/(4La_N + Sm_N)] \tag{3}$$

$$Ce\ \ anomaly = \log\left[Ce_N/\left(La_N^{2/3} \times Nd_N^{1/3}\right)\right] \tag{4}$$

where N indicates the PAAS-normalized concentration. For the Eu anomaly, the Eu/Sm ratio is commonly considered if data on Gd are absent (Dubinin, 2004). However, with the advent of analytical techniques that allow for measurement of all 14 naturally occurring REEs, such as ICP-MS, Ce and Eu anomalies are now commonly and precisely calculated based on neighboring REE (de Baar et al., 1983; Bau and Dulski, 1996; Johannesson et al., 2006; Marmolejo-Rodríguez et al., 2007):

$$Ce\ \ anomaly = \log[2Ce_N/(La_N + Pr_N)] \tag{5}$$

$$Eu\ \ anomaly = \log[2Eu_N/(Sm_N + Gd_N)] \tag{6}$$

$$Eu\ \ anomaly = \log\left[Eu_N/(Sm_N \times Gd_N)^{0.5}\right]. \tag{7}$$

In this study, we adopted Eqs. (5) and (6) to calculate Ce and Eu anomalies, respectively. However, we calculated Ce and Eu anomalies using all of the equations above and found no differences of significance between the various methods (Supplementary Table 3). The presence of a positive La anomaly, as found in modern seawater and some marine sediments, can complicate calculation of the Ce anomaly (de Baar et al., 1991). Where a La anomaly is suspected, the Ce anomaly can be evaluated by calculating the value of Pr/Pr*:

$$Pr/Pr^* = 2Pr_N/(Ce_N + Nd_N). \tag{8}$$

Where Pr/Pr* is equal to 1, no Ce anomaly exists; Pr/Pr* > 1.0 and < 1.0 indicate negative and positive Ce anomalies, respectively (Bau and Dulski, 1996; Webb and Kamber, 2000). Although the majority of the study samples do not exhibit a La anomaly, we have calculated Pr/Pr* as a check on Ce anomalies determined by Eq. (5). One point to note is that "negative" and "positive" anomalies correspond to values of < 1.0 and > 1.0, respectively, when calculated on an arithmetic basis (e.g., Eq. (8)) and to values of < 0 and > 0 when calculated on a logarithmic basis (e.g., Eqs. (2)–(7)).

3. Results and discussion

3.1. REE compositions: intra- and inter-core comparisons

Because study cores WPD-03 and WPD-12 exhibit similar elemental concentration patterns within the LDM facies, we present only the results of core WPD-03 to illustrate downcore variations in geochemistry (see Supplementary Table 2 for large datasets). The depth profiles of opal, total REEs ($\sum$REE), Ti, Mn/Ti, P/Ti, Fe/Ti, Al/Ti and Ba/Ti from core WPD-03 are shown in Fig. 2. Here, the vertical profile of $\sum$REE concentrations can be taken as representative of those of individual REEs due to the similarity of their downcore patterns. The concentration of opal, which ranges from 1.5% to 75.9% and reaches peak values in the middle to upper portion of the LDM, dominates downcore compositional changes. Downcore changes in major elements, trace elements, and REEs vary inversely with opal, reflecting their strong dilution by BSi. Ti-normalized ratios for individual REEs, light REEs (LREE, La to Nd), middle REEs (MREE, Sm to Tb), heavy REEs (HREE, Dy to Lu) and $\sum$REE in the LDM-03, DC, PC and LDM-12 are illustrated in Fig. 3.

Ti-normalized individual REE concentrations are not obviously different among the LDM-03, DC and PC (Fig. 3). Accordingly, the concentrations of LREE, MREE, HREE and $\sum$REE normalized to Ti do not discriminate well among the three lithostratigraphic units above. Moreover, Ti-normalized ratios for the LDM-03 are also close to those of the LDM-12. The relatively invariant ratios shown by Ti-normalized individual REE, LREE, MREE, HREE and $\sum$REE both within and between the study cores indicate that, although biogenic opal diluted the detrital REE fraction, it made little direct contribution to bulk REE concentrations (Elderfield et al., 1981; Pattan et al., 2005; Tanaka et al., 2007). In general, diatom frustules have low REE concentrations (Piper, 1974a; Elderfield et al., 1981), which may explain the limited contribution that diatoms made to bulk REE abundances in the study units.

To understand the geochemical behavior of REEs in the study cores, the mean and range of REE concentrations in the samples of LDM-03, DC, PC and LDM-12 were normalized to PAAS (Fig. 4). On the whole, all sample REE patterns in the four lithostratigraphic units above display nearly the same characteristics: MREE and HREE are strongly enriched compared with LREE, and MREE is slightly enriched relative to HREE. These enrichment patterns are also confirmed by $(Eu/La)_N$, $(Yb/La)_N$ and $(Eu/Yb)_N$ ratios, the means of which are almost all more than unity in the four lithostratigraphic units above (Table 2). Although the REE patterns of LDM-03 and LDM-12 are the same as those of DC and PC, close inspection reveals some slight differences. First, both LDM-03 and LDM-12 exhibit small positive Ce anomalies, whereas DC exhibits a variably negative or positive Ce anomaly and PC a weak negative Ce anomaly (Fig. 4). Second, the DC and PC always exhibit a moderate positive Eu anomaly, whereas the LDM-03 and LDM-12 show a weaker Eu anomaly that is variably positive or negative (Fig. 4). Third, in core WPD-03, the enrichments of MREE and HREE relative to LREE and of MREE relative to HREE gradually decrease through time during the successive deposition of the PC, DC and LDM facies (Fig. 4), a pattern documented also by changes in the ratios of $(Eu/La)_N$, $(Yb/La)_N$ and $(Eu/Yb)_N$ (Table 2). These slight differences among facies do not result from REE contributions by biogenic opal but, rather, mainly from variations in post-depositional uptake of REEs (see Sections 3.2 and 3.3).

3.2. Potential carrier phases of REEs

The concentrations and patterns of REEs are not controlled by the content of biogenic opal in the study cores (see Section 3.1), indicating that the REE composition of the LDM is unrelated to blooms of the diatom *E. rex*. Other processes that can potentially influence the enrichment and depletion of REEs in marine sediments include detrital input, authigenic removal, and early diagenesis (Sholkovitz, 1988). Determining the carrier phases (mineral or organic) of REEs can provide insights into the relative importance of such processes for REE accumulation in sediments. In this study, we explore potential carrier phases of REEs in the study cores by (1) assessing REE enrichment or depletion relative to expected detrital REE concentrations based on PAAS, (2) calculating excess (authigenic) REE concentrations, and (3) comparing REE patterns for the authigenic fraction of the study samples with typical PAAS-normalized REE patterns for possible authigenic host phases.

LREE concentrations in the LDM-03, DC, PC, and LDM-12 are close to those of PAAS on a Ti-normalized basis (Fig. 3), suggesting that the LREE fraction is carried primarily by detrital phases. This inference is also supported by the PAAS-normalized REE patterns for the detrital and authigenic fractions, because the sample/PAAS ratios of LREEs in the detrital fraction are around 1 order of magnitude greater than those of LREEs in the authigenic fraction (Fig. 5). MREEs and HREEs

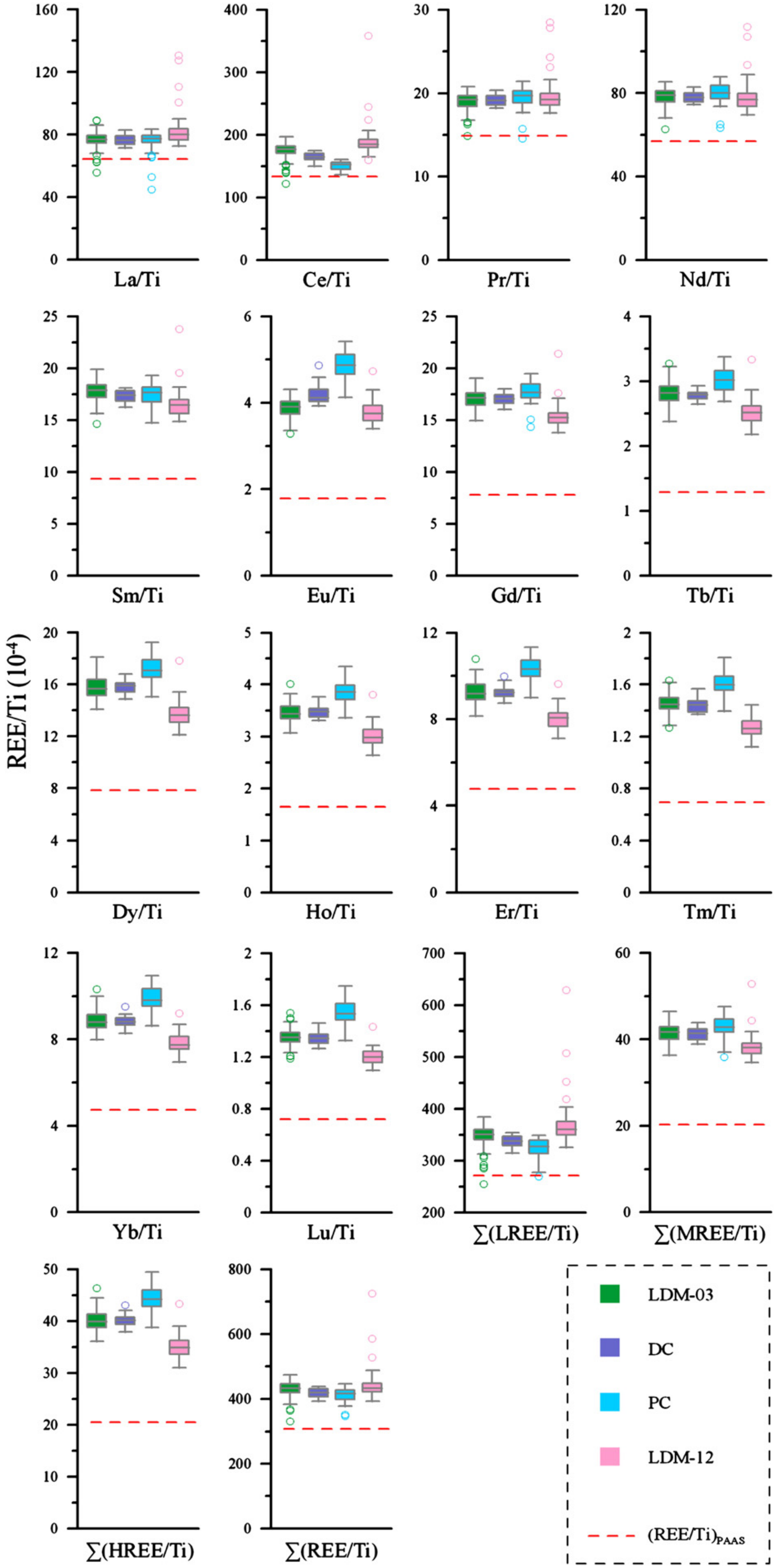
REE/Ti (10⁻⁴)
La/Ti
0
40
80
120
160
Ce/Ti
0
100
200
300
400
Pr/Ti
0
10
20
30
Nd/Ti
0
40
80
120
Sm/Ti
0
5
10
15
20
25
Eu/Ti
0
2
4
6
Gd/Ti
0
5
10
15
20
25
Tb/Ti
0
1
2
3
4
Dy/Ti
0
4
8
12
16
20
Ho/Ti
0
1
2
3
4
5
Er/Ti
0
4
8
12
Tm/Ti
0
0.4
0.8
1.2
1.6
2
Yb/Ti
0
4
8
12
Lu/Ti
0
0.4
0.8
1.2
1.6
2
∑(LREE/Ti)
200
300
400
500
600
700
∑(MREE/Ti)
0
20
40
60
∑(HREE/Ti)
0
10
20
30
40
50
∑(REE/Ti)
0
200
400
600
800
🟩 LDM-03
🟦 DC
🟦 PC
🟪 LDM-12
(REE/Ti)PAAS

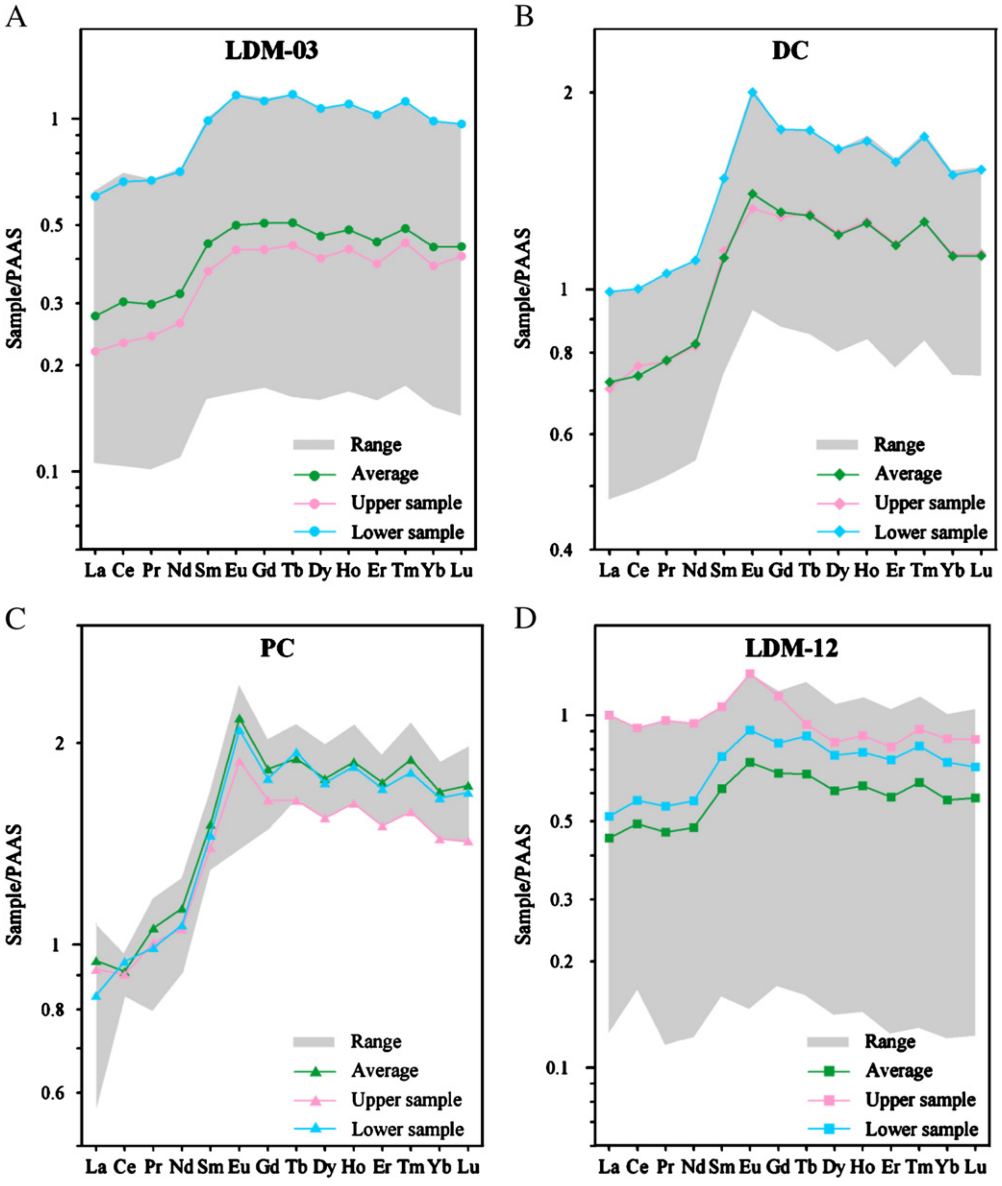

Fig. 4. PAAS-normalized REE distribution patterns for (A) LDM-03, (B) DC, (C) PC, and (D) LDM-12. The gray field shows the full range of variation in REE values for each unit; the green curve represents the average value for each REE, and the pink and blue curves give representative examples of REE distributions for samples from the upper and lower half of each unit, respectively. See Fig. 2 for abbreviations.

are strongly enriched relative to the PAAS standard (Fig. 3), reflecting a combination of detrital and authigenic sources (Fig. 5). Lack of REE fractionation in the detrital fraction is suggested by an absence of correlations of $(Eu/La)_N$, $(Yb/La)_N$ and $(Eu/Yb)_N$ with Al/Ti (Fig. 6A).

Substantial enrichment of MREEs and HREEs over LREEs in LDM-03, DC, PC, and LDM-12 is indicative of the preferential removal of the former elements from seawater to the sediment (Pattan et al., 2005). Seawater is HREE enriched and has a more-or-less uniform pattern of greater REE abundance with higher atomic numbers (Fig. 7A; Elderfield and Greaves, 1982). The distinct HREE enrichment relative to PAAS that is observed in LDM-03, DC, PC, and LDM-12 may thus be indicative of large hydrogenous fraction resulting from REE uptake directly from seawater. However, the study samples exhibit significantly greater MREE enrichment, as reflected in $(Eu/Yb)_N$ ratios of 1.1–1.3 (Table 2), than seawater, which has $(Eu/Yb)_N$ ratios of 0.2–0.4. Thus, an additional source of MREEs is necessary to account for REE distribution patterns in LDM-03, DC, PC, and LDM-12.

One interesting question is which authigenic phases control the enrichment of MREEs and HREEs. The potential authigenic phases in the core sediments are associated with Mn, P, Fe, Ba (Fig. 2), and redox-sensitive and sulfide-forming trace elements (not shown). First, the authigenic accumulation of redox-sensitive and sulfide-forming elements cannot account for MREE and HREE enrichment due to their trace amounts and absence of positive correlations with $(Eu/La)_N$, $(Yb/La)_N$ and $(Eu/Yb)_N$ (Fig. 6B, C). Second, marine barite does not show an enrichment of MREEs and HREEs relative to LREEs, although published studies have reported some variation in its REE pattern (Fig. 7B; Piper, 1974a; Guichard et al., 1979). Third,

Fig. 3. Variability of Ti-normalized ratios for individual REEs as well as for sums of the light, middle, heavy, and total REEs in cores WPD-03 and WPD-12 by lithofacies (DC, PC, and LDM). Each box-and-whisker plot shows the median (horizontal line), 25th and 75th percentile values (bar), and minimum and maximum values (vertical line) for a REE/Ti ratio; circles represent extreme values (outliers). See Fig. 2 for abbreviations.

Table 2
Range and average of $(Eu/La)_N$, $(Yb/La)_N$ and $(Eu/Yb)_N$ for LDM-03, DC, PC, and LDM-12.

Units[a]	$(Eu/La)_N$		$(Yb/La)_N$		$(Eu/Yb)_N$	
	Range	Average	Range	Average	Range	Average
LDM-03	1.53–2.66	1.80	1.40–2.23	1.57	0.98–1.27[b]	1.15
DC	1.74–2.13	1.93	1.43–1.72	1.56	1.18–1.34	1.24
PC	2.01–3.32	2.33	1.57–2.88	1.81	1.16–1.37	1.29
LDM-12	0.62–1.83[c]	1.62	0.86–1.42[d]	1.29	1.16–1.53	1.28

[a] n = 81, 24, 32 and 50 in LDM-03, DC, PC and LDM-12, respectively.
[b] Only one sample with $(Eu/Yb)_N < 1.0$.
[c] Only one sample with $(Eu/La)_N < 1.0$.
[d] Only four samples with $(Yb/La)_N < 1.0$.

it is unlikely that organic materials control the MREE and HREE enrichments because of the low TOC contents (0.08–0.35%) of the study sediments (Xiong et al., in review).

Phosphates commonly display highly variable REE patterns due to variations in their source, age and origin (Shields and Stille, 2001). MREE enrichment is characteristic of old phosphate and biogenic apatite in many marine formations (Grandjean-Lécuyer et al., 1993; Kidder et al., 2003), probably owing to strong REE fractionation during uptake by phosphatic phases (Byrne et al., 1996; Kidder et al., 2003) although possibly as a consequence of pre-Cenozoic seawater having a MREE-enriched composition (Grandjean-Lécuyer et al., 1993). Younger marine authigenic phosphates tend to show strong HREE enrichment (relative to MREEs and LREEs), mirroring distribution patterns seen in modern northwest Pacific bottom waters (Fig. 7A; Piper et al., 1988, Pattan et al., 2005). A lack of positive correlation of P/Ti with Ca/Ti ($r = -0.43$) indicates that P in the study units is not primarily associated with either biogenic apatite or authigenic phosphate. Rather, positive covariation of P/Ti with Mn/Ti ($r = +0.90$, $p(\alpha) < 0.01$) suggests that P may be present primarily adsorbed onto Mn-oxyhydroxides (Glenn et al., 1994; Jarvis et al., 1994).

MREE enrichment is also a striking feature observed in marine authigenic Mn phases, such as ferromanganese nodules and crusts (Nath et al., 1992; Kuhn et al., 1998; Takahashi et al., 2000) (Fig. 7B), Fe–Mn coatings (Palmer, 1985; Palmer and Elderfield, 1986), and manganese micronodules (Addy, 1979). Therefore, the pattern of MREE enrichment observed in the study cores probably has an origin in co-precipitation with Mn and/or Fe oxyhydroxides.

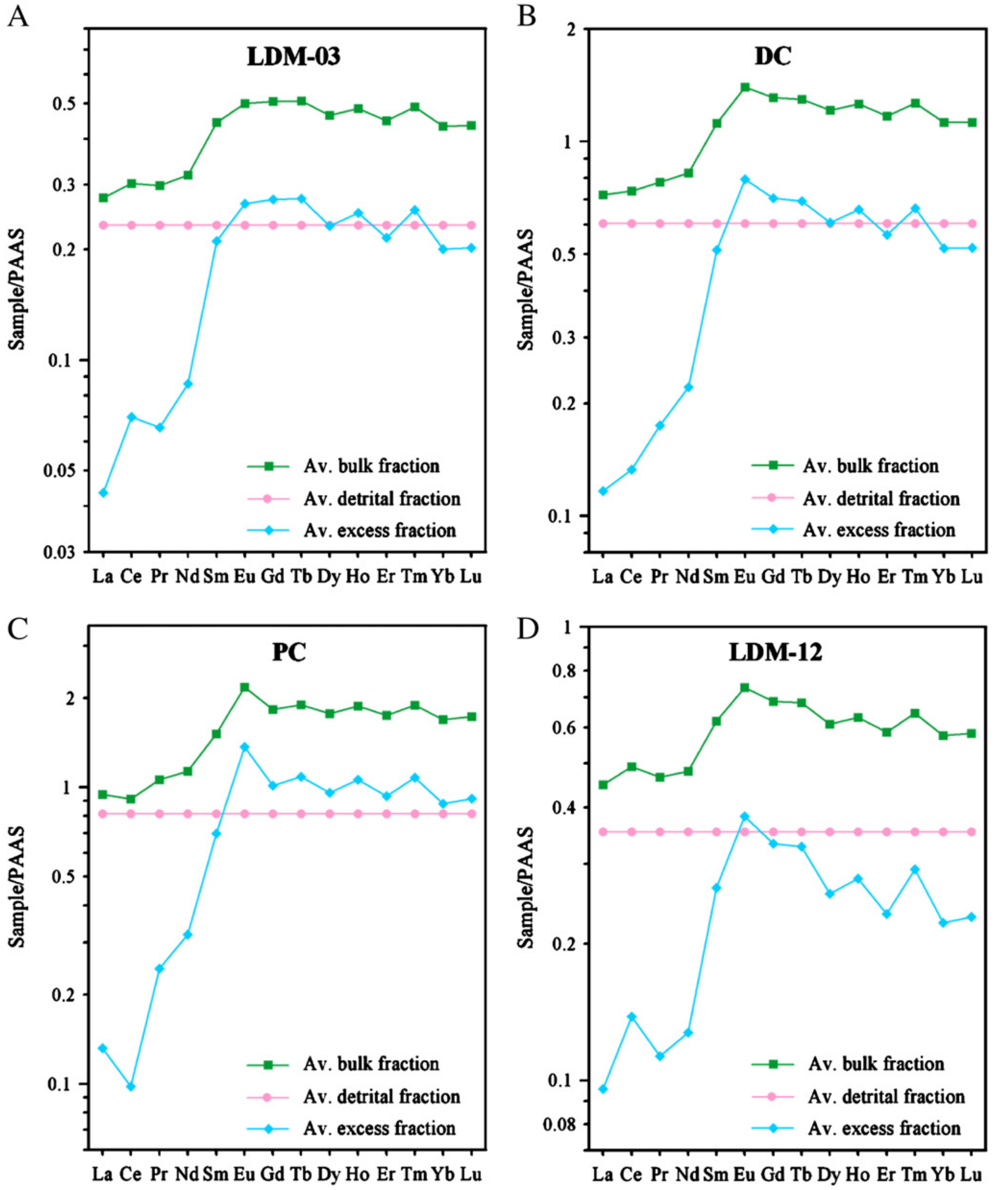

Fig. 5. PAAS-normalized REE patterns of the bulk, detrital, and excess (authigenic) fractions for (A) LDM-03, (B) DC, (C) PC, and (D) LDM-12. The excess fraction was calculated per Eq. (1) of the text. See Fig. 2 for abbreviations.

This inference is supported by positive correlations of $(Eu/La)_N$ and $(Eu/Yb)_N$ with Mn/Ti (Fig. 6D). We also note that Fe/Ti shows poor correlations with $(Eu/La)_N$, $(Yb/La)_N$ and $(Eu/Yb)_N$ (Fig. 6E), suggesting that MREE enrichment is associated with Mn oxyhydroxides rather than Fe authigenic phases (i.e., Fe oxyhydroxides in PC and DC, and Fe sulfides in LDM).

To summarize, LREEs are dominantly carried by the detrital fraction of the two study cores, whereas MREEs and HREEs are derived from a combination of detrital and authigenic sources. Strong MREE enrichment (relative to LREE and HREE) is indicative of a large REE contribution from Mn oxyhydroxides, while HREE enrichment (relative to LREE rather than MREE) is suggestive of a small contribution from authigenic phosphate. These results are consistent with the findings of Takebe (2005) that REEs in Pacific deep-sea sediments are carried mainly by eolian dust from Asia, carbonate fluorapatites, and Mn oxides.

3.3. Ce and Eu anomalies

3.3.1. Redox chemistry of Ce and Eu

Ce and Eu are the only redox-sensitive REEs. In suboxic/anoxic marine environments Ce^{+4} is reduced to Ce^{3+}, in which state it behaves similarly to other trivalent REEs, resulting in minimal fractionation and little or no Ce anomaly in REE distributions. In oxic marine environments Ce^{+3} is oxidized to Ce^{4+}, in which state it tends to be rapidly scavenged by colloids in suspension (German and Elderfield, 1989; German et al., 1991) or by Fe and Mn oxyhydroxides in the sediment (Alibo and Nozaki, 1999; Nozaki, 2009). Such scavenging imparts a distinct negative Ce anomaly to seawater. Consequently, the Ce-anomaly proxy has great potential for reconstruction of the redox conditions prevailing at the time of sediment deposition (Wang et al., 1986; Liu et al., 1988; Yang et al., 1999; Girard and Lécuyer, 2002; Kato et al., 2002; Kakuwa and Matsumoto, 2006; Feng et al., 2008; Azmy et al., 2009). However, various factors, e.g., detrital input, diagenetic alteration, and REE exchange between pore water and sediment, may obscure the original Ce anomaly (MacLeod and Irving, 1996). Pattan et al. (2005) emphasized the importance of identifying the mineral phases responsible for the Ce anomaly in the bulk sediment in order to validate its utility for analysis of bottomwater redox conditions. Some studies have explored the diagenetic processes responsible for REE redistribution in the sediment and noted caveats regarding use of the Ce anomaly as a paleoseawater redox proxy (Murray et al., 1991; Holser, 1997; Mazumdar et al., 1999; Shields and Stille, 2001; Kidder et al., 2003). MacLeod and Irving (1996) pointed out that the Ce anomaly often covaries with paleoredox conditions but that too much uncertainty exists at present to permit its use as a stand-alone redox indicator. Furthermore, de Baar et al. (1988) and German and Elderfield (1990) suggested that the Ce anomaly does not provide an instantaneous measure of ambient redox conditions but reflects the time-integrated redox history of the sediment instead. In view of these uncertainties, use of the Ce anomaly as a paleoredox proxy in marine sediments must be approached cautiously.

Theoretically, Eu is oxidized to Eu^{3+} in oxic environments and converts to Eu^{2+} in anoxic environments (Brookins, 1989). However, reduction of Eu^{3+} to Eu^{2+} is favored only at high temperatures (i.e., >250 °C) (Sverjensky, 1984); thus, Eu anomalies are most common in hydrothermal fluids, magmas, and igneous and metamorphic minerals (Dubinin, 2004). On the other hand, reduction to Eu^{+2} is rare in low-temperature, near-surface environments such as the ocean except under extremely reducing conditions (Sverjensky, 1984). Only a few cases of development of Eu anomalies have been reported from low-temperature environments, mostly in association with diagenesis in organic-rich, sulfate-reducing facies (MacRae et al., 1992; Martinez-Ruiz et al., 1999).

3.3.2. Relationships between Ce anomaly and redox conditions

In core WPD-03, the depth profile of the Ce anomaly exhibits subtle but systematic changes in relation to the three main lithostratigraphic units (Fig. 8A). The PC, DC, and LDM-03 show weak negative, nearly neutral, and weak positive Ce anomalies, respectively (Fig. 8A). Except for three positive outliers, all PC samples show negative Ce anomalies varying from −0.079 to −0.019, with an average of −0.050. The predominance of negative anomalies in the PC is consistent with observations by Toyoda et al. (1990) that red pelagic clay samples from low-latitude Pacific sites generally show negative Ce anomalies, whereas those from high-latitude sites show positive anomalies.

Negative Ce anomalies in the study sediments cannot be attributed to the detrital fraction, which generally does not show a Ce anomaly (Piper, 1974a). Rather, the negative Ce anomaly is probably hosted by the authigenic fraction of the sediment (Fig. 5C), which includes Fe and Mn oxyhydroxides and phosphates (Fig. 2; see Section 3.2). Marine authigenic Fe–Mn oxyhydroxides of hydrogenous origin commonly show positive Ce anomalies owing to the oxidation of Ce^{3+} in seawater to Ce^{4+} and its subsequent uptake as CeO_2 by metalliferous nodules (Piper, 1974b; de Carlo, 1991; Nath et al., 1992; Takahashi et al., 2000) (Fig. 7B). In contrast, hydrothermal Fe–Mn deposits typically exhibit negative Ce anomalies (Elderfield and Greaves, 1981; Kuhn et al., 1998). Because the Fe–Mn oxyhydroxides in the study units are of hydrogenous origin (Xu et al., 2007), the negative Ce anomalies in the PC cannot be attributed to the REE fraction associated with Fe–Mn oxyhydroxides.

Young marine authigenic phosphate also is typically characterized by a negative Ce anomaly (Piper, 1974a, b; Piper et al., 1988; MacLeod and Irving, 1996) (Fig. 7A). Toyoda et al. (1990) and Toyoda and Masuda (1991) suggested that, in samples of Pacific pelagic sediments, a positive Ce anomaly is caused by preferential scavenging of Ce from seawater to the sediment while a negative Ce anomaly is incorporated with the phosphate phase. The magnitude of the negative Ce anomaly may vary as a function of the source of phosphate: authigenic phosphate typically has a moderate negative anomaly whereas biogenic phosphate has a strong negative anomaly (MacLeod and Irving, 1996). We note that the negative Ce anomaly of the PC is relatively weak (Fig. 8A) and, hence, potentially consistent with the inference of a small contribution from authigenic phosphate (see Section 3.2). Further, the negative correlation between the Ce anomaly and P/Ti (Fig. 9A) might be interpreted as evidence of an authigenic phosphate phase with a negative Ce anomaly in the study sediments, although it might also be the product of an incidental correlation resulting from adsorption of P onto Mn-oxyhydroxides (see Section 3.2).

The LDM-03 yields a persistently weak positive Ce anomaly ranging from 0 to 0.052, with an average of 0.024 (excepting three negative outliers; Fig. 8A). Although the LDM-03 is dominated by biogenic opal, diatoms generally have a negative Ce anomaly and low REE abundances (Piper, 1974a; Elderfeld et al., 1981) (Fig. 7A), indicating that REE patterns in the LDM are probably controlled by authigenic phases. Although a positive Ce anomaly can result from the presence of hydrogenous Fe–Mn oxyhydroxides, Mn is present in very low concentrations in the LDM-03 (except for the uppermost 45 cm of the LDM; Fig. 2). Smectite formed by the weathering of submarine volcanic rocks and glass also has a positive Ce anomaly (Desprairies and Bonnot-Courtois, 1980; Tlig and Steinberg, 1982) (Fig. 7A). Nevertheless, the contribution of smectite to the positive Ce anomaly of the LDM is probably minor because the Ce anomaly does not correlate with smectite abundance (Fig. 9B). Thus, unlike the lithologically sourced negative Ce anomaly of the PC, the positive Ce anomaly of the LDM-03 is likely to represent a hydrogenous (i.e. seawater) signal.

REE investigations of suboxic/anoxic marine and lacustrine systems, such as Chesapeake Bay, Black Sea, Saanich Inlet (British Columbia), Cariaco Trench, Bannock Basin (eastern Mediterranean Sea), and Lake

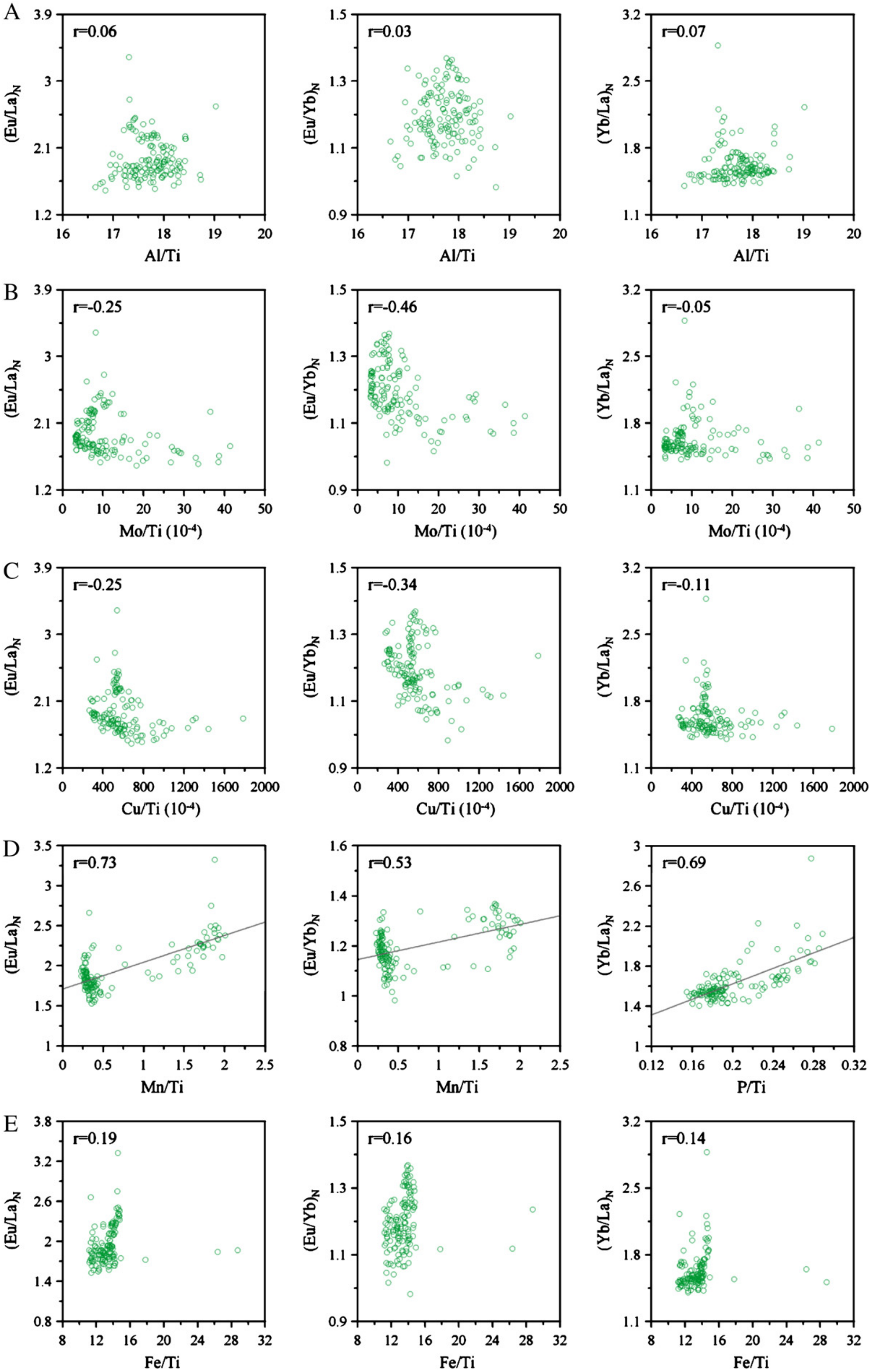
A
r=0.06
r=0.03
r=0.07
(Eu/La)N
(Eu/Yb)N
(Yb/La)N
Al/Ti
B
r=-0.25
r=-0.46
r=-0.05
Mo/Ti (10-4)
C
r=-0.25
r=-0.34
r=-0.11
Cu/Ti (10-4)
D
r=0.73
r=0.53
r=0.69
Mn/Ti
P/Ti
E
r=0.19
r=0.16
r=0.14
Fe/Ti

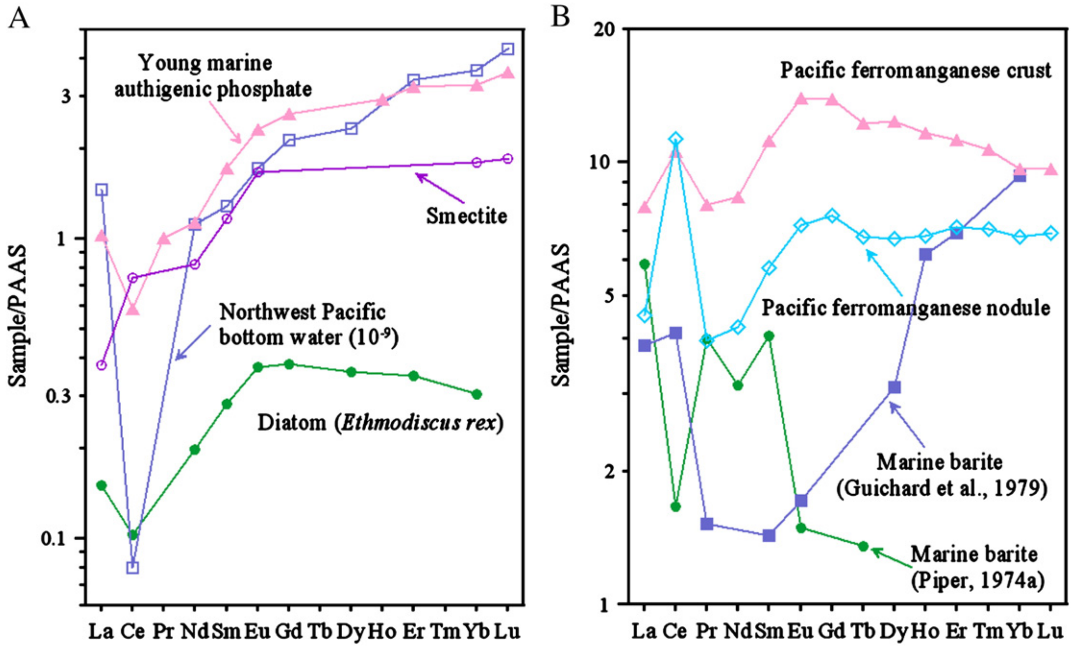

Fig. 7. Typical PAAS-normalized REE patterns of modern marine sediments and seawater. Data sources: Pacific ferromanganese crusts and nodules (Takahashi et al., 2000), smectite (formed by the weathering of submarine volcanic materials) (Desprairies and Bonnot-Courtois, 1980), marine barite (Piper, 1974a; Guichard et al., 1979), young marine authigenic phosphate (Piper et al., 1988), Northwest Pacific bottom water (Piepgras and Jacobsen, 1992), and diatoms (*Ethmodiscus rex*) (Elderfield et al., 1981).

Vanda (Antarctica), suggest that REE cycling generally occurs at the oxic/suboxic (or oxic/anoxic) interface and is closely associated with redox cycling of Mn oxyhydroxides in the water column (de Baar et al., 1988; Sholkovitz and Elderfield, 1988; German and Elderfield, 1989; German et al., 1991; Sholkovitz et al., 1992; Schijf et al., 1995; de Carlo and Green, 2002). Reductive dissolution of Mn oxyhydroxides in the deeper (subchemoclinal) water mass results in the (usually weak) preferential release of Ce^{3+} relative to its trivalent-only REE neighbors, reducing or eliminating the negative Ce anomaly produced in oxic water masses (de Baar et al., 1988; German et al., 1991; de Carlo and Green, 2002). In such reducing environments, preferentially released Ce^{3+} can be scavenged by settling particulates and removed to sediments (Sholkovitz et al., 1994; Kato et al., 2002), sometimes yielding a positive Ce anomaly in bulk sediments. Since the LDM was exposed to suboxic bottom waters during its deposition and sulfidic anoxic porewaters subsequently (Xiong et al., in review), the weak positive Ce anomaly of this unit is likely to have had an origin through the process of Mn-oxyhydroxide redox cycling.

Which phases in the LDM record the positive Ce anomaly? Fig. 5A and D demonstrate that the positive Ce anomaly in the LDM is exclusively incorporated in the authigenic fraction. We infer that barite and Fe sulfides, which are the two main authigenic phases in the LDM (Fig. 2), may have contributed to the development of the positive Ce anomaly. Although the barite formation process is thought to occur mainly in the upper water column, where most organic matter decays, it can potentially take place at any water depth, including at the sediment–water interface (Paytan and Griffith, 2007). Formation of barite may have occurred at the sediment–water interface of the study sites because sulfidic anoxic conditions existed during LDM deposition as a result of an increased flux of organic matter to the seafloor (Xiong et al., in review). Barite forming at the sediment–water interface may have scavenged Ce^{3+} from porewater and seawater, leading to the observed positive Ce anomaly (Fig. 8A). This inference is supported by the strong positive correlation of the Ce anomaly with Ba/Ti (Fig. 9C).

Uptake of Ce^{3+} by Fe sulfides is also possible, as coprecipitation of REEs with metal sulfides has been reported (Brookins, 1989; Schijf et al., 1995; Chaillou et al., 2006). For example, this process was invoked to account for dissolved REE distributions in the anoxic brines of the Bannock Basin (eastern Mediterranean Sea; Schijf et al., 1995). Fe sulfides are typically the dominant metal sulfides in marine systems, yet the Ce anomaly and Fe/Ti do not show a good correlation in the LDM (Fig. 9D). In addition, Fe_{xs} (average ~0.60%) only represents a minor fraction (~34%) of total Fe (average ~1.78%) (Fig. 2), suggesting that Fe sulfides are present at low levels in the LDM. Based on the considerations above, Fe sulfides are probably not the main carrier phase for the positive Ce anomaly in the LDM.

The DC shows Ce anomaly values intermediate between those of the LDM-03 and PC, with a range from −0.040 to 0.013 and an average of −0.007 (Fig. 8A). As a transitional lithostratigraphic unit, the Ce anomaly in the DC probably reflects the mixed effects of the lithogenic signal in the PC and the authigenic signal in the LDM. Therefore, the value of the Ce anomaly in the DC depends on the relative influence of these inputs.

3.3.3. Relationships between Eu anomaly and redox conditions

Previous analytical studies have shown that care must be taken in the interpretation of positive Eu anomalies measured by ICP-MS, due to various Ba-compound interferences (Dulski, 1994; Jiang et al., 2007). The excellent linear but *negative* correlation between the Eu anomaly and Ba/Ti in the WPD-03 core (Fig. 9E) suggests that the Eu anomaly in the study sediments is not an instrumental artifact and can be used as a paleoenvironmental indicator (Shields and Stille, 2001; Jiang et al., 2007). Positive Eu anomalies of sediments in the eastern Philippine Sea have been shown to result from the presence of volcanogenic materials (Xu et al., 2008). On this basis,

Fig. 6. Crossplots of $(Eu/La)_N$, $(Eu/Yb)_N$ and $(Yb/La)_N$ versus (A) Al/Ti, (B) Mo/Ti, (C) Cu/Ti, (D) Mn/Ti or P/Ti, and (E) Fe/Ti for core WPD-03. For all graphs, n = 137 and the probabilities of alpha errors p(α) ≥0.05 and ≥0.01 correspond to correlation coefficients r^2 of ≤0.17 and ≤0.22, respectively.

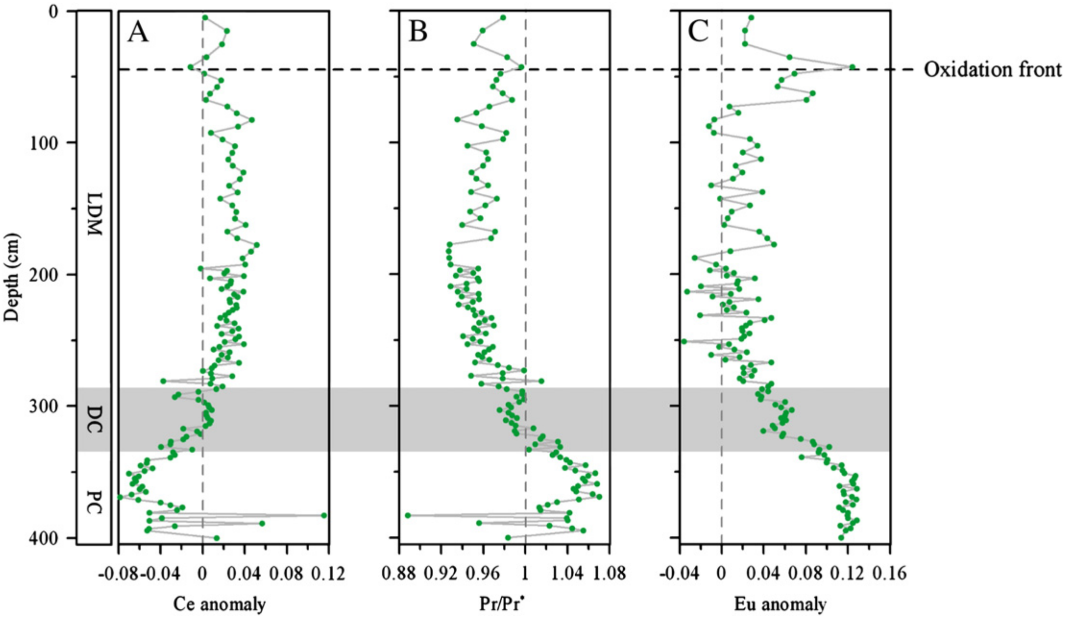

Fig. 8. Vertical profiles of (A) Ce anomaly, (B) Pr/Pr*, and (C) Eu anomaly in core WPD-03. Ce and Eu anomalies were calculated per Eqs. (5) and (6) and Pr/Pr* per Eq. (8). Pr/Pr* is a check on Ce anomalies that is independent of possible La anomalies; see Section 2.3 for details. The dashed vertical lines show the zero value for each anomaly. The dashed horizontal line shows the position of the active oxidation front (Xiong et al., in review).

Eu anomalies in the study sediments could be interpreted in terms of variable contributions of volcanogenic materials. However, the smaller Eu anomaly of the LDM-03 and DC relative to the PC is unlikely to represent decreased volcanogenic inputs because the depth profiles of lithogenic elements (i.e., Al/Ti and Cr/Ti) imply that the detrital flux to the site of core WPD-03 was constant during deposition of the 4-m-thick study interval (Fig. 2). Here, we propose that the smaller Eu anomaly in the LDM-03 and DC relative to the PC (Fig. 8C) was the result of the reduction of excess Eu^{3+} of volcanogenic materials to Eu^{2+} under extremely reducing porewater conditions (Sverjensky, 1984; MacRae et al., 1992; Martinez-Ruiz et al., 1999). Although Eu^{2+} can substitute for Ba^{2+} in barite by virtue of its similarity in size and charge (Guichard et al., 1979), this process appears not to have operated in the LDM-03 and DC, because there is no positive correlation between the Eu anomaly and Ba/Ti (Fig. 9E). This observation suggests that excess Eu^{2+} was not re-incorporated into the sediments and thus supports our inference with regard to the origin of Eu anomalies in the LDM-03 and DC.

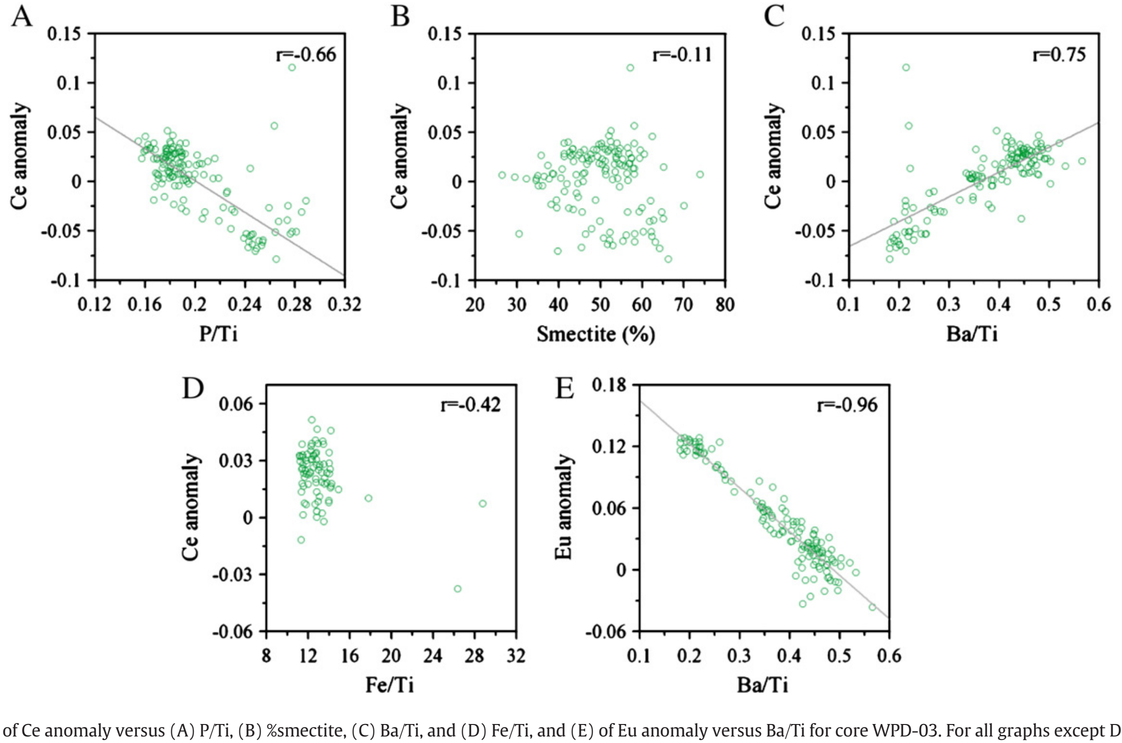

Fig. 9. Crossplots of Ce anomaly versus (A) P/Ti, (B) %smectite, (C) Ba/Ti, and (D) Fe/Ti, and (E) of Eu anomaly versus Ba/Ti for core WPD-03. For all graphs except D, n = 137 and the probabilities of alpha errors p(α) ≥0.05 and ≥0.01 correspond to correlation coefficient r^2 of ≤0.17 and ≤0.22, respectively. For graph D, n = 81 and the probabilities of alpha errors p(α) ≥0.05 and ≥0.01 correspond to correlation coefficients r^2 ≤0.22 and ≤0.28, respectively.

3.3.4. Diagenetic influences on Ce and Eu anomalies

The role of early diagenetic processes in controlling REE distributions in marine sediments has received limited attention (Pattan and Banakar, 1997; Caetano et al., 2009), especially with regard to diagenetic influences on Ce and Eu anomalies (German and Elderfield, 1990; MacRae et al., 1992; Martinez-Ruiz et al., 1999; Shields and Stille, 2001). In core WPD-03, the Ce anomaly profile exhibits a weak minimum and the Eu anomaly profile a strong maximum around a depth of 45 cm, which coincides with the depth to which an active oxidation front penetrated (Fig. 8) (Xiong et al., in review). This relationship suggests that downward movement of the oxidation front resulted in some degree of diagenetic remobilization of Ce and Eu within the sediment, producing local features in the depth profiles.

Excess Ce^{3+} and Eu^{2+} existed in sediment porewaters due to their respective reduction under sulfidic anoxic conditions during the LDM deposition. These cations would have moved upward along concentration gradients (MacRae et al., 1992; Pattan and Banakar, 1997) and been re-oxidized to CeO_2 and Eu^{3+} upon reaching the oxidation front at a depth of 45 cm (Fig. 8). Eu that is oxidized to Eu^{3+} was directly incorporated into the sediment, yielding a local maximum in the depth profile. A similar mechanism was invoked by MacRae et al. (1992) to explain the development of a positive Eu anomaly in Pleistocene muds of the Amazon deep-sea fan. The behavior of Ce in the diagenetic environment was probably more complex: oxidized CeO_2 may have been taken up by LDM sediments, but at the same time barite may have scavenged reduced Ce^{3+} in the porewater. These two processes would have counteracting effects on the Ce anomaly, yielding a compromise value that reflects neither strong depletion nor enrichment of Ce at the active oxidation front.

3.4. Redox conditions and primary productivity during the LGM

Although the conditions of formation of *E. rex* diatom mats are still under debate (see review in Romero and Schmieder, 2006), mass accumulations of this diatom in tropical ocean sediments are generally related to strong oceanic stratification, while *E. rex* oozes in subtropical marine sediments are mainly associated with frontal zones (i.e., interfaces between ocean water masses). As a ‘shade flora’ (Kemp et al., 2000), *E. rex* is adapted to grow in subsurface waters with low-light conditions and can migrate vertically between the deep for nutrient utilization and the surface for photosynthesis. This survival strategy is especially successful in stably stratified water masses (Villareal, 1993). Because the study area in the eastern Philippine Sea is not proximal to any frontal zones, the occurrence of LDMs in the study core is more likely to be linked to the ocean stratification. Stratification of the eastern Philippine Sea during the LGM could have trapped nutrients (i.e., nitrate and silicic acid) in sub-photic-zone (i.e., intermediate) water masses that were accessible by populations of *E. rex* owing to their ability to migrate vertically in the water column. This scenario reconciles evidence for high levels of primary productivity in the eastern Philippine Sea during the LGM (Xiong et al., in review) with blooms of *E. rex*, which are generally associated with water-column stratification and, hence, reduced vertical mixing in tropical settings.

Redox conditions in the water column result from the interaction of lateral ventilation of deep waters, vertical overturn (i.e., thermohaline circulation), and primary productivity rates (Arthur and Sageman, 1994). High primary productivity rates and enhanced water-column stratification favor more reducing bottom waters, but strong lateral ventilation of deep waters can counteract these factors. Deep ocean circulation and deep water ventilation in the eastern Philippine Sea during the LGM are poorly understood. In view of the depth of the seafloor in the study area (5250 m), deep circulation is mainly controlled by the Lower Circumpolar Water (LCPW) (Siedler et al., 2004), which originates from intermingling of North Atlantic Deep Water (NADW) and Antarctic Bottom Water (AABW) (Kawabe et al., 2003). The rate of NADW formation during the LGM may have been higher than during the Holocene, as shown by model simulations (Kitoh et al., 2001; Hewitt et al., 2003) and paleoceanographic data (Veum et al., 1992; McCave et al., 1995). However, AABW production during the LGM is more poorly constrained. Pudsey and Howe (1998) inferred stronger flow of the Antarctic Circumpolar Current (ACC) during the LGM than during the Holocene on the basis of sediment grain-size data from the Scotia Sea, which may be an indication of enhanced AABW production during the LGM. These considerations suggest that deep-water ventilation in the study area should not have been lower, and was possibly higher, during the LGM than at present.

Geochemical evidence suggests that eastern Philippine Sea bottomwaters were more reducing during the LGM than today. Evidence for redox changes is provided by Ce and Eu anomalies, which suggest a gradual development of more reducing conditions during DC deposition and sustained anoxia during LDM formation (Fig. 8). Other evidence for redox changes is provided by trace-metal profiles, which show modest to locally strong levels of enrichment in the LDM of both study units (Xiong et al., in review). Although the degree of trace-metal enrichment is lower than in laminated diatomaceous sediments of Saanich Inlet, British Columbia (Morford et al., 2001; Russell and Morford, 2001) or Plio-Pleistocene Mediterranean sapropels (Warning and Brumsack, 2000; Brumsack, 2006), uptake of trace metals may have been influenced by the low permeability of laminated *E. rex* mats and consequent limited advection of waters across the sediment–water interface. In view of evidence for enhanced ventilation of eastern Philippine Sea bottomwaters due to greater advection of LCPW during the LGM (see above), the more reducing conditions inferred during LDM formation are likely to have been the result of increased primary productivity rates and higher sinking fluxes of organic matter. This inference is consistent with evidence for higher primary productivity rates in the form of %opal (Fig. 2) and TOC and Ba_{xs} concentrations (Xiong et al., in review).

The occurrence of laminated sediments is common in anoxic facies owing to suppression of bioturbation under low-oxygen conditions (Behl and Kennett, 1996; Bull et al., 2000). However, in the last two decades, LDMs have been recovered from several deep-sea settings where bottom waters are well oxygenated (Kemp and Baldauf, 1993; Bodén and Backman, 1996; King et al., 1998; Pike and Kemp, 1999). Preservation of laminae in these diatom oozes was not attributed to anoxic conditions but, rather, to rapid deposition of robust diatom mats and their intrinsic meshwork, which prevented or restricted benthic activity (Kemp and Baldauf, 1993; Pike and Kemp, 1999). On the contrary, our results show that LDMs formation in the eastern Philippine Sea coincided with more reducing bottomwater conditions during the LGM, indicating that controls on LDM formation are more complicated and varied than previously thought. Apart from the high accumulation rates and low permeability of LDMs (Kemp and Baldauf, 1993; Pike and Kemp, 1999), we suggest that elevated primary productivity and its effects on benthic redox conditions may also be important influences on the formation of LDMs in some settings.

Paleoceanographic changes in the eastern Philippine Sea during the late Pleistocene are not well understood due to the absence of carbonate fossils such as foraminifera and coccolithophores. The massive accumulation of LDMs in this region during the LGM (Zhai et al., 2009) may provide significant insights regarding contemporaneous changes in environmental conditions. As an oligotrophic open-ocean setting, the modern eastern Philippine Sea is characterized by low primary and export productivity (Berger and Wefer, 1991). However, our results indicate that high primary productivity rates were associated with blooms of the diatom *E. rex* during the LGM, which is different from the productivity pattern at present. Enhanced primary productivity during LDM deposition caused suboxic bottomwaters owing to a high organic carbon sinking flux, consistent with the deeper respired carbon pool in the glacial equatorial and subarctic Pacific Ocean (Jaccard et al., 2009; Bradtmiller et al., 2010). Our results from the eastern Philippine Sea thus support inferences of increased carbon storage at a basinwide scale in the glacial deep Pacific Ocean. Enhanced storage of carbon in the deep Pacific may have played an important role in modulating atmospheric CO_2 variation during Pleistocene glacial–interglacial cycles (Jaccard et al., 2009; Bradtmiller et al., 2010).

4. Conclusions

(1) LDM-03, DC, PC, and LDM-12 show similar REE patterns reflecting strong enrichment of MREE and HREE over LREE, and slight enrichment of MREE over HREE. Meanwhile, the four lithostratigraphic units above exhibit relatively uniform Ti-normalized ratios for individual REEs. These observations imply that biogenic opal in the LDM contributed very little to the abundance and distribution pattern of REEs in bulk core sediments and, thus, that REE compositions are not influenced by blooms of the diatom *E. rex*. LREEs are dominantly associated with detrital materials, whereas MREEs and HREEs have been selectively enriched by adsorption onto Mn oxyhydroxides and authigenic phosphates, respectively.

(2) The presence of minor authigenic phosphates imparts a weak negative Ce anomaly to the PC, resulting in a signature that does not conform with the oxic conditions of PC deposition. Enhanced scavenging of reduced aqueous Ce^{3+} by barite in a sulfidic anoxic environment produced a positive Ce anomaly in the LDM that accurately reflects the strongly reducing conditions of LDM deposition. Ce anomalies ranging from negative to positive in the DC may reflect the combination of effects associated with Ce geochemical behavior in the LDM and PC.

(3) The positive Eu anomaly in core WPD-03 is derived from feldspar-bearing volcanogenic materials. The smaller Eu anomaly in the LDM and DC relative to that in the PC is attributed to the reduction of Eu^{3+} to Eu^{2+} and its subsequent release to sediment porewaters under strongly reducing conditions rather than to the decreased input of detrital materials.

(4) In view of increased ventilation of eastern Philippine Sea deep waters by Lower Circumpolar Water during the LGM, persistent bottomwater suboxia was probably the result of high primary productivity rates associated with blooms of the diatom *E. rex*. Such blooms may have been the product of enhanced water-column stratification in the eastern Philippine Sea, favoring a 'shade flora' capable of vertical migration and producing a 'deep chlorophyll maximum.' These conditions persisted throughout the interval of LDM formation from ~26 to 20 kyr B.P.

(5) Enhanced primary productivity and more reducing bottomwaters during LDM deposition is likely to have increased the respired carbon pool in the deep eastern Philippine Sea. Increased carbon storage during glacial stages not only in the eastern Philippine Sea but also across the deep Pacific Ocean may have been an important factor in modulation of atmospheric CO_2 variation during Pleistocene glacial–interglacial cycles.

Supplementary materials related to this article can be found online at doi:10.1016/j.chemgeo.2011.12.012.

Acknowledgments

We thank Uwe Brand and two anonymous reviewers for their constructive comments. This study was supported by the National Natural Science Foundation of China (Grant No. 40776031 and No. 41106042) and National Fundamental Research and Development Planning Project (Grant No. 2007CB815903). TJA thanks the U.S. National Science Foundation for support.

References

Addy, S.K., 1979. Rare earth element patterns in manganese nodules and micronodules from northwest Atlantic. Geochimica et Cosmochimica Acta 43, 1105–1115.

Alibo, D.S., Nozaki, Y., 1999. Rare earth elements in seawater: particle association, shale-normalization, and Ce oxidation. Geochimica et Cosmochimica Acta 63 (3/4), 363–372.

Arthur, M.A., Sageman, B.B., 1994. Marine black shales: depositional mechanisms and environments of ancient deposits. Annual Review of Earth and Planetary Sciences 22, 499–551.

Azmy, K., Sylvester, P., de Oliveira, T.F., 2009. Oceanic redox conditions in the Late Mesoproterozoic recorded in the upper Vazante Group carbonates of São Francisco Basin, Brazil: evidence from stable isotopes and REEs. Precambrian Research 168, 259–270.

Bau, M., Dulski, P., 1996. Distribution of yttrium and rare-earth elements in the Penge and Kuruman iron-formations, Transvaal Supergroup, South Africa. Precambrian Research 79, 37–55.

Behl, R.J., Kennett, J.P., 1996. Brief interstadial events in the Santa Barbara Basin, NE Pacific, during the past 60 kyr. Nature 379, 243–246.

Berger, W.H., Wefer, G., 1991. Productivity of the glacial ocean: discussion of the iron hypothesis. Limnology and Oceanography 36 (8), 1899–1918.

Bodén, P., Backman, J., 1996. A laminated sediment sequence from northern North Atlantic Ocean and its climatic record. Geology 24, 507–510.

Bradtmiller, L.I., Anderson, R.F., Sachs, J.P., Fleisher, M.Q., 2010. A deeper respired carbon pool in the glacial equatorial Pacific Ocean. Earth and Planetary Science Letters 299, 417–425.

Brookins, D.G., 1989. Aqueous geochemistry of rare earth elements. In: Lipin, B.R., McKay, G.A. (Eds.), Geochemistry and Mineralogy of Rare Earth Elements. Mineralogical Society of America, Reviews in Mineralogy, vol. 21, pp. 201–225.

Brumsack, H.-J., 2006. The trace metal content of recent organic carbon-rich sediments: implications for Cretaceous black shale formation. Palaeogeography, Palaeoclimatology, Palaeoecology 232, 344–361.

Bull, D., Kemp, A.E.S., Weedon, G.P., 2000. A 160-k.y.-old record of El Nino-Southern Oscillation in marine production and coastal runoff from Santa Barbara Basin, California, USA. Geology 28, 1007–1010.

Byrne, R.H., Liu, X., Schijf, J., 1996. The influence of phosphate coprecipitation on rare earth distributions in natural waters. Geochimica et Cosmochimica Acta 60, 3341–3346.

Caetano, M., Prego, R., Vale, C., de Pablo, H., Marmolejo-Rodríguez, J., 2009. Record of diagenesis of rare earth elements and other metals in a transitional sedimentary environment. Marine Chemistry 116, 36–46.

Chaillou, G., Anschutz, P., Lavaux, G., Blanc, G., 2006. Rare earth elements in the modern sediments of the Biscay (France). Marine Chemistry 100, 39–52.

de Baar, H.J.W., Bacon, M.P., Brewer, P.G., 1983. Rare-earth distributions with a positive Ce anomaly in the West North Atlantic Ocean. Nature 301, 324–327.

de Baar, H.J.W., German, C.R., Elderfield, H., van Gaans, P., 1988. Rare earth element distributions in anoxic waters of the Cariaco Trench. Geochimica et Cosmochimica Acta 52, 1203–1219.

de Baar, H.J.W., Schijf, J., Byrne, R.H., 1991. Solution chemistry of the rare earth elements in seawater. European Journal of Solid State and Inorganic Chemistry 28, 357–373.

de Carlo, E.H., 1991. Paleoceanographic implications of rare earth element variability within a Fe–Mn crust from the central Pacific Ocean. Marine Geology 98, 449–467.

de Carlo, E.H., Green, W.J., 2002. Rare earth elements in the water column of Lake Vanda, McMurdo Dry Valleys, Antarctica. Geochimica et Cosmochimica Acta 66 (8), 1323–1333.

De Deckker, P., Gingele, F.X., 2002. On the occurrence of the giant diatom *Ethmodiscus rex* in an 80-ka record from a deep-sea core, southeast of Sumatra, Indonesia: implications for tropical oceanography. Marine Geology 183, 31–43.

Desprairies, A., Bonnot-Courtois, C., 1980. Relation entre la composition des smectites d'alteration sous-marine et leur cortege de terres rares. Earth and Planetary Science Letters 48, 124–130.

Dubinin, A.V., 2004. Geochemistry of rare earth elements in the ocean. Lithology and Mineral Resources 39 (4), 289–307.

Dulski, P., 1994. Interferences of oxide, hydroxide and chloride analyte species in the determination of rare earth elements in geological samples by inductively coupled plasma-mass spectrometry. Fresenius' Journal of Analytical Chemistry 350, 194–203.

Elderfield, H., Greaves, M.J., 1981. Negative cerium anomalies in the rare earth element patterns of oceanic ferromanganese nodules. Earth and Planetary Science Letters 55, 163–170.

Elderfield, H., Greaves, M.J., 1982. The rare earth elements in seawater. Nature 296, 214–219.

Elderfield, H., Hawkesworth, C.J., Greaves, M.J., Calvert, S.E., 1981. Rare earth element geochemistry of oceanic ferromanganese nodules and associated sediments. Geochimica et Cosmochimica Acta 45, 513–528.

Feng, D., Chen, D.F., Peckmann, J., 2008. Rare earth elements in seep carbonates as tracers of variable redox conditions at ancient hydrocarbon seeps. Terra Nova 21 (1), 49–56.

German, C.R., Elderfield, H., 1989. Rare earth elements in Saanich Inlet, British Columbia, a seasonally anoxic basin. Geochimica et Cosmochimica Acta 53, 2561–2571.

German, C.R., Elderfield, H., 1990. Application of the Ce anomaly as a paleoredox indicator: the ground rules. Paleoceanography 5 (5), 823–833.

German, C.R., Holliday, B.P., Elderfield, H., 1991. Redox cycling of rare earth elements in the suboxic zone of the Black Sea. Geochimica et Cosmochimica Acta 55, 3553–3558.

Gingele, F.X., De Deckker, P., Girault, A., Guichard, F., 2002. History of the south java current over the past 80 ka. Palaeogeography, Palaeoclimatology, Palaeoecology 183, 247–260.

Gingele, F.X., Schmieder, F., 2001. Anomalous South Atlantic lithologies confirm global scales of unusual mid Pleistocene climate excursion. Earth Planetary Science Letter 186, 93–101.

Girard, C., Lécuyer, C., 2002. Variations in Ce anomalies of conodonts through the Frasnian/Famennian boundary of Poland (Kowala-Holy Cross Mountains): implications for the redox state of seawater and biodiversity. Palaeogeography, Palaeoclimatology, Palaeoecology 181, 299–311.

Glenn, C.R., Föllmi, K.B., Riggs, S.R., Baturin, G.N., Grimm, K.A., Trappe, J., Abed, A.M., Galli-Oliver, C., Garrison, R.E., Dyin, A., Jehl, C., Rohrich, V., Sadaquah, R., Schiderlowski, M., Sheldon, R.E., Seigmund, H., 1994. Phosphorus and phosphorites: sedimentology and environments of formation. Eclogae Geologica Helvetiae 87, 747–788.

Grandjean-Lécuyer, P., Feist, R., Albarède, F., 1993. Rare earth elements in old biogenic apatites. Geochimica et Cosmochimica Acta 57, 2507–2514.

Guichard, F., Church, T.M., Treuil, M., Jaffrezic, H., 1979. Rare earth in barites: distribution and effects on aqueous partitioning. Geochimica et Cosmochimica Acta 43, 983–997.

Haley, B.A., Klinkhammer, G.P., McManus, J., 2004. Rare earth elements in pore waters of marine sediments. Geochimica et Cosmochimica Acta 68 (6), 1265–1279.

Hewitt, C.D., Stouffer, R.J., Broccoli, A.J., Mitchell, J.F.B., Valdes, P.J., 2003. The effect of ocean dynamics in a coupled GCM simulation of the Last Glacial Maximum. Climate Dynamics 20, 203–218.

Holser, W., 1997. Evaluation of the application of rare-earth elements to paleoceanography. Palaeogeography, Palaeoclimatology, Palaeoecology 132, 309–323.

Jaccard, S.L., Galbraith, E.D., Sigman, D.M., Haug, G.H., Francois, R., Pedersen, T.F., Dulski, P., Thierstein, H.R., 2009. Subarctic Pacific evidence for a glacial deepening of the oceanic respired carbon pool. Earth and Planetary Science Letters 277, 156–165.

Jarvis, I., Burnett, W.C., Nathan, J., Almbaydin, F.S.M., Attia, A.K.M., Castro, L.N., Flicoteau, R., Hilmy, M.E., Husein, V., Quitwanah, A.A., Serjani, A.A., Zanin, Y., 1994. Phosphorite geochemistry: state of the art and environmental concerns. Eclogae Geologica Helvetiae 87, 643–700.

Jiang, S.Y., Zhao, H.X., Chen, Y.Q., Yang, T., Yang, J.H., Ling, H.F., 2007. Trace and rare earth element geochemistry of phosphate nodules from the lower Cambrian black shale sequence in the Mufu Mountain of Nanjing, Jiangsu province, China. Chemical Geology 244, 584–604.

Johannesson, K.H., Hawkins Jr., D.L., Cortés, A., 2006. Do Archean chemical sediments record ancient seawater rare earth element patterns? Geochimica et Cosmochimica Acta 70, 871–890.

Kakuwa, Y., Matsumoto, R., 2006. Cerium negative anomaly just before the Permian and Triassic boundary event—the upward expansion of anoxia in the water column. Palaeogeography, Palaeoclimatology, Palaeoecology 229, 335–344.

Kato, Y., Nakao, K., Isozaki, Y., 2002. Geochemistry of Late Permian to Early Triassic pelagic cherts from southwest Japan: implications for an oceanic redox change. Chemical Geology 182, 15–34.

Kawabe, M., Fujio, S., Yanagimoto, D., 2003. Deep-water circulation at low latitudes in the western North Pacific. Deep-Sea Research I 50, 631–656.

Kemp, A.E.S., Baldauf, J.G., 1993. Vast Neogene laminated diatom mat deposits from the eastern equatorial Pacific Ocean. Nature 362, 141–143.

Kemp, A.E.S., Pearce, R.B., Grigorov, I., Rance, J., Lange, C.B., Quilty, P., Salter, I., 2006. Production of giant marine diatoms and their export at oceanic frontal zones: implications for Si and C flux from stratified oceans. Global Biogeochemical Cycles 20, GB4S04. doi:10.1029/2006GB002698.

Kemp, A.E.S., Pike, J., Pearce, R.B., Lange, C.B., 2000. The "Fall Dump"—a new perspective on the role of a "shade flora" in the annual cycle of diatom production and exportation. Deep-Sea Research II 47, 2129–2154.

Kidder, D.L., Krishnaswamy, R., Mapes, R.H., 2003. Elemental mobility in phosphatic shales during concretion growth and implications for provenance analysis. Chemical Geology 198, 335–353.

King, S.C., Murray, J.W., Kemp, A.E.S., 1998. Palaeoenvironments of deposition of Neogene laminated diatom mat deposits from the eastern equatorial Pacific from studies of benthic foraminifera (Sites 844, 849, 851). Marine Micropalaeontology 35, 161–177.

Kitoh, A., Murakami, S., Koide, H., 2001. A simulation of the last glacial maximum with a coupled atmosphere–ocean GCM. Geophysical Research Letters 28, 2221–2224.

Kuhn, T., Bau, M., Blum, N., Halbach, P., 1998. Origin of negative Ce anomalies in mixed hydrothermal–hydrogenetic Fe–Mn crusts from the Central Indian Ridge. Earth and Planetary Science Letters 163, 207–220.

Lacan, F., Jeandel, C., 2001. Tracing Papua New Guinea imprint on the central Equatorial Pacific Ocean using neodymium isotopic compositions and rare earth element patterns. Earth and Planetary Science Letters 186, 497–512.

Lerche, D., Nozaki, Y., 1998. Rare earth elements of sinking particulate matter in the Japan Trench. Earth and Planetary Science Letters 159, 71–86.

Liu, Y.G., Miah, M.R.U., Schmitt, R.A., 1988. Cerium: a chemical tracer for paleo-oceanic redox conditions. Geochimica et Cosmochimica Acta 52, 1361–1371.

MacLeod, K.G., Irving, A.J., 1996. Correlation of cerium anomalies with indicators of paleoenvironment. Journal of Sedimentary Research 66 (5), 948–955.

MacRae, N.D., Nesbitt, H.W., Kronberg, B.I., 1992. Development of a positive Eu anomaly during diagenesis. Earth and Planetary Science Letters 109, 585–591.

Marmolejo-Rodríguez, Prego, R., Meyer-Willerer, A., Shumilin, E., Sapozhnikov, D., 2007. Rare earth elements in iron oxy-hydroxide rich sediments from the Marabasco River–Estuary System (pacific coast of Mexico) REE affinity with iron and aluminium. Journal of Geochemical Exploration 94, 43–51.

Martinez-Ruiz, F., Ortega-Huertas, M., Palomo, I., 1999. Positive Eu anomaly development during diagenesis of the K/T boundary ejecta layer in the Agost section (SE Spain): implications for trace-element remobilization. Terra Nova 11 (6), 290–296.

Mazumdar, A., Banerjee, D.M., Schidlowski, M., Balaram, V., 1999. Rare-earth elements and stable isotope geochemistry of early Cambrian chert–phosphorite assemblages from the Lower Tal Formation of the Krol Belt (Lesser Himalaya, India). Chemical Geology 156, 275–297.

McCave, I.N., Manighetti, B., Beveridge, N.A.S., 1995. Circulation in the glacial North Atlantic inferred from grain-size measurements. Nature 374, 149–152.

Morad, S., Felitsyn, S., 2001. Identification of primary Ce-anomaly signatures in fossil biogenic apatite: implication for the Cambrian oceanic anoxia and phosphogenesis. Sedimentary Geology 143, 259–264.

Morford, J.L., Russell, A.D., Emerson, S., 2001. Trace metal evidence for changes in the redox environment associated with the transition from terrigenous clay to diatomaceous sediments, Saanich Inlet, BC. Marine Geology 174, 355–369.

Mortlock, R.A., Froelich, P.N., 1989. A simple method for the rapid-determination of biogenic opal in pelagic marine-sediments. Deep-Sea Research I 36, 1415–1426.

Munksgaard, N.C., Lim, K., Parry, D.L., 2003. Rare earth elements as provenance indicators in Norh Australian estuarine and coastal marine sediments. Estuarine, Coastal and Shelf Science 57, 399–409.

Murray, R.W., Buchholtz ten Brink, M.R., Brumsack, H.J., Gerlach, D.C., Russ III, G.P., 1991. Rare earth elements in Japan sea sediments and diagenetic behavior of Ce/Ce*: results from ODP Leg 127. Geochimica et Cosmochimica Acta 55, 2453–2466.

Murray, R.W., Leinen, M., Isern, A.R., 1993. Biogenic flux of Al to sediment in the central equatorial Pacific Ocean: evidence for increased productivity during glacial periods. Paleoceanography 8, 651–670.

Nath, B.N., Balaram, V., Sudhakar, M., Plüger, W.L., 1992. Rare earth element geochemistry of ferromanganese deposits from the Indian Ocean. Marine Chemistry 38, 185–208.

Nozaki, Y., 2009. Rare earth elements and their isotopes. In: Steele, J., Thorpe, S., Turekian, K. (Eds.), Encyclopedia of Ocean Sciences. Academic Press, New York, pp. 653–665.

Palmer, M.R., 1985. Rare earth elements in foraminifera tests. Earth and Planetary Science Letters 73, 285–298.

Palmer, M.R., Elderfield, H., 1986. Rare earth elements and neodymium isotopes in ferromanganese oxide coatings of Cenozoic foraminifera from the Atlantic Ocean. Geochimica et Cosmochimica Acta 50, 409–417.

Pattan, J.N., Banakar, V.K., 1997. Diagenetic remobilization of rare earth elements in a sediment core from the central Indian Basin. Indian Journal of Marine Sciences 26, 341–344.

Pattan, J.N., Pearce, N.J.G., Mislankar, P.G., 2005. Constraints in using cerium-anomaly of bulk sediments as an indicator of paleo bottom water redox environment: a case study from the Central Indian Ocean Basin. Chemical Geology 221, 260–278.

Paytan, A., Griffith, E.M., 2007. Marine barite: recorder of variations in ocean export productivity. Deep-Sea Research II 54, 687–705.

Piepgras, D.J., Jacobsen, S.B., 1992. The behavior of rare earth elements in seawater: precise determination of variations in the North Pacific water column. Geochimica et Cosmochimica Acta 56, 1851–1862.

Pike, J., Kemp, A.E.S., 1999. Diatom mats in Gulf of California sediments: implications for the paleoenvironmental interpretation of laminated sediments and silica burial. Geology 27, 311–314.

Piper, D.Z., 1974a. Rare earth elements in the sedimentary cycle: a summary. Chemical Geology 14, 285–304.

Piper, D.Z., 1974b. Rare earth elements in ferromanganese nodules and other marine phases. Geochimica et Cosmochimica Acta 38, 1007–1022.

Piper, D.Z., Baedecker, P.A., Crock, J.G., Burnett, W.C., Loebner, B.J., 1988. Rare-earth elements in the phosphatic-enriched sediment of the Peru Shelf. Marine Geology 80, 269–285.

Piper, D.Z., Perkins, R.B., Rowe, H.D., 2007. Rare-earth elements in the Permian Phosphoria Formation: paleo proxies of ocean geochemistry. Deep-Sea Research II 54, 1396–1413.

Pudsey, C.J., Howe, J.A., 1998. Quaternary history of the Antarctic Circumpolar Current: evidence from the Scotia Sea. Marine Geology 148, 83–112.

Romero, O., Schmieder, F., 2006. Occurrence of thick *Ethmodiscus* oozes associated with a terminal Mid-Pleistocene Transition event in the oligotrophic subtropical South Atlantic. Palaeogeography, Palaeoclimatology, Palaeoecology 235, 321–329.

Russell, A.D., Morford, J.L., 2001. The behavior of redox-sensitive metals across a laminated–massive–laminated transition in Saanich Inlet, British Columbia. Marine Geology 174, 341–354.

Schijf, J., de Baar, H.J.W., Millero, F.J., 1995. Vertical distributions and speciation of dissolved rare earth elements in the anoxic brines of Bannock Basin, eastern Mediterranean Sea. Geochimica et Cosmochimica Acta 59 (16), 3285–3299.

Shields, G., Stille, P., 2001. Diagenetic constraints on the use of cerium anomalies as paleoseawater redox proxies: an isotope and REE study of Cambrian phosphorites. Chemical Geology 175, 29–48.

Sholkovitz, E.R., 1988. Rare earth elements in the sediments of the North Atlantic Ocean, Amazon Delta, and East China Sea: reinterpretation of terrigenous input patterns to the oceans. American Journal of Science 288, 236–281.

Sholkovitz, E.R., Elderfield, H., 1988. Cycling of dissolved rare earth elements in Chesapeake Bay. Global Biogeochemical Cycles 2 (2), 157–176.

Sholkovitz, E.R., Landing, W.M., Lewis, B.L., 1994. Ocean particle chemistry: the fractionation of rare earth elements between suspended particles and seawater. Geochimica et Cosmochimica Acta 58 (6), 1567–1579.

Sholkovitz, E.R., Shaw, T.J., Schneider, D.L., 1992. The geochemistry of rare earth elements in the seasonally anoxic water column and porewaters of Chesapeake Bay. Geochimica et Cosmochimica Acta 56, 3389–3402.

Siedler, G., Holfort, J., Zenk, W., Muller, T.J., Csernok, T., 2004. Deep-water flow in the Mariana and Caroline Basins. Journal of Physical Oceanography 34, 566–581.

Sverjensky, D.A., 1984. Europium redox equilibria in aqueous solution. Earth and Planetary Science Letters 67, 70–78.

Takahashi, Y., Shimizu, H., Usui, A., Kagi, H., Nomura, M., 2000. Direct observation of tetravalent cerium in ferromanganese nodules and crusts by X-ray-absorption near-edge structure (XANES). Geochimica et Cosmochimica Acta 64 (17), 2929–2935.

Takebe, M., 2005. Carriers of rare earth elements in Pacific deep-sea sediments. Journal of Geology 113, 201–215.

Tanaka, K., Akagawa, F., Yamamoto, K., Tani, Y., Kawabe, T., Kawai, T., 2007. Rare earth element geochemistry of Lake Baikal sediment: its implication for geochemical response to climate change during the Last Glacial/Interglacial transition. Quaternary Science Reviews 26, 1362–1368.

Taylor, S.R., McClennan, S.M., 1985. The Continental Crust: Its Composition and Evolution. Blackwell Scientific Publications, Oxford.

Tlig, S., Steinberg, M., 1982. Distribution of rare earth elements (REE) in size fractions of recent sediments of the Indian Ocean. Chemical Geology 37, 317–333.

Toyoda, K., Masuda, A., 1991. Chemical leaching of pelagic sediments: identification of the carrier of Ce anomaly. Geochemical Journal 25, 95–119.

Toyoda, K., Nakamura, Y., Masuda, A., 1990. Rare earth elements of Pacific pelagic sediments. Geochimica et Cosmochimica Acta 54, 1093–1103.

Veum, T., Jansen, E., Arnold, M., Beyer, I., Duplessy, J.-C., 1992. Water mass exchange between the North Atlantic and the Norwegian Sea during the past 28,000 years. Nature 356, 783–785.

Villareal, T.A., 1993. Abundance of the giant diatom *Ethmodiscus* in the Southwest Atlantic Ocean and Central Pacific Gyre. Diatom Research 8, 171–177.

Wang, Y.L., Liu, Y.G., Schmitt, R.A., 1986. Rare earth geochemistry of south Atlantic deep sediments: Ce anomaly change at 54 My. Geochimica et Cosmochimica Acta 50, 1337–1355.

Warning, B., Brumsack, H.-J., 2000. Trace metal signatures of eastern Mediterranean sapropels. Palaeogeography, Palaeoclimatology, Palaeoecology 158, 293–309.

Webb, G.E., Kamber, B.S., 2000. Rare earth elements in Holocene reefal microbialites: a new shallow seawater proxy. Geochimica et Cosmochimica Acta 64, 1557–1565.

Wilde, P., Quinby-Hunt, M.S., Erdtmann, B.D., 1996. The whole-rock cerium anomaly: a potential indicator of eustatic sea-level changes in shales of the anoxic facies. Sedimentary Geology 101, 43–53.

Xiong, Z.F., Li, T.G., Algeo, T.J., Nan, Q.Y., Zhai, B., Lu, B., in review. Major and trace metals and biogenic components of diatom mats from tropical West Pacific: implications for redox conditions and paleoproductivity. Marine Geology.

Xu, Z.K., Li, A.C., Jiang, F.Q., Li, T.G., Meng, Q.Y., Jin, N., 2007. Paleoenvironment evolution of the East Philippine Sea recorded in the new-type ferromanganese crust since the terminal Late Miocene. Science in China Series D: Earth Sciences 50 (8), 1179–1188.

Xu, Z.K., Li, A.C., Jiang, F.Q., Xu, F.J., 2008. Geochemical character and material source of sediments in the eastern Philippine Sea. Chinese Science Bulletin 53 (6), 923–931.

Yang, J.D., Sun, W.G., Wang, Z.H., Xue, Y.S., Tao, X.C., 1999. Variations in Sr and C isotopes and Ce anomalies in successions from China: evidence for the oxygenation of Neoproterozoic seawater? Precambrian Research 93, 215–233.

Yoder, J.A., Ackleson, S.G., Barber, R.T., Flament, P., Balch, W.M., 1994. A line in the sea. Nature 371, 689–692.

Zhai, B., Li, T.G., Chang, F.M., Cao, Q.Y., 2009. Vast laminated diatom mat deposits from the west low-latitude Pacific Ocean in the last glacial period. Chinese Science Bulletin 54, 4529–4533.